Yanez, J., & Veiga-López, F. (2021). Theoretical analysis of the condensation of combustion products in thin gaseous layers. Physics of Fluids, 33(8), 083601.

DOI: https://doi.org/10.1063/5.0056831

Theoretical analysis of the condensation of combustion products in thin gaseous layers

Jorge Yanez[1] and Fernando Veiga-López[2]
[1)]*Institute for Thermal Energy Technology and Safety, Karlsruhe Institute of Technology, 76131 Karlsruhe, Germany*
[2)]*Institut Pprime, UPR 3346 CNRS, ISAE–ENSMA, Futuroscope–Chasseneuil Cedex, FRA 86961, France*

(*E-mail: jyanezescanciano@gmail.com)

In this paper, a theoretical analysis of the condensation of combustion products in narrow gaps between planar plates is performed. The investigation is motivated by the empirical results shown by F. Veiga López, Flame propagation in narrow channels, Ph.D. thesis, Carlos III University of Madrid (2020), and the lack of a theoretical description directly applicable to them. In these experiments, he describes how discontinuous condensed water films appeared on the walls of the combustion chamber, forming dry/wet stripes parallel to the flame front at the products region.

The formulation developed here is derived from a general approach for condensation, which is simplified considering the conditions of high-temperature combustion products. Notably, the liquid phase disappears from the system of equations, which exclusively contains the gaseous phase. The expressions resulting are analytical, simple and easy to interpret. They allow us to understand qualitatively the effects of the main physical phenomena of the process, which is described by the interaction between heat exchange, mass transfer, the thermodynamic conditions and the velocity of the combustion products.

The construct is subsequently utilized to perform numerical parametric studies, to analyze the influence of two main parameters of the problem: gap thickness and flame velocity. Despite the relative simplicity of the model, it predicts similar condensation-vaporization-condensation cycles to those observed at the laboratory.

I. INTRODUCTION AND MOTIVATION

Recent experiments performed by Veiga[1] show an unusual behaviour of near-stoichiometric hydrogen-air premixed flames. Burning such mixtures, characteristic zebra patterns appear (Fig. 1): dark stripes of condensed combustion products are followed by lighter areas without liquid. The flames oscillate, recording pressure waves with maximum peaks of around 6.5 kPa at 300 Hz.

Having a look into the literature, one can easily find that flames propagating in narrow geometries undergo familiar instabilities,[2–4]. In most of cases those instabilities are: a) hydrodynamic,[5–7]; b) thermodiffusive[8–10]; c) thermoacoustic[11–15]; d) Rayleigh-Taylor[16] .

From our standpoint, the unstable response of the flame cannot be directly linked to these instability mechanisms. In particular, the influence of acoustic effects was discarded as the frequency of the oscillations could not be related to any acoustic mode of the combustion chamber. Likewise, it did not present a precise peak but a wide band of frequencies. Furthermore, the flame shape is very smooth with some cells probably due to the Darrieus-Landau instability. But it does not show the characteristic lobes of the thermoacoustic instability. In our opinion, the peculiar trace left by the combustion products behind the front connect the flame dynamics to change of phase phenomena.

Regarding condensation, we note that steam machinery was basic for the Industrial Revolution and it is still widely used in boilers, condensers, etc.[17,18]. Thus, the analysis of change-of-phase in tubes is a classic problem and has been consequently thoroughly studied[19–22]. Numerous authors derived different models to understand heat and mass transfer occurring at the interface between a liquid and its vapor. The focus of previous analyses was commonly centered in the condensation of low-temperature flows within the frame of a determined industrial application.

Of significance for this study is the fact that multi-phase flows are also subjected to instabilities. An interesting review of this topic can be found in[23]. We only summarize here some relevant facts. Firstly, we realize that instabilities could happen for evaporating or condensing streams. Secondly, the mechanisms associated to condensation and evaporation are thought to be completely different. Thirdly, we note that instabilities could be related to the condensation of one of the components of the multi-phase gaseous mixture[24]. Additionally, it is also relevant that these instabilities not only apply to large scale machinery, but also to small-scale systems[25]. Small-scale condensation-driven unstable flows appear mostly due to the pressure drop at the tubes[26] and the well-studied Density Wave Oscillations[27].

Back on the literature relevant to combustion, it is surprising that not many studies are focused on condensation. To the best of our knowledge, only di Benedetto et al.[28] consider phase-change phenomena on what they called *Rapid-Phase Transition*. Additionally, Kuznetsov and Grüne[29] provided a brief overview of the effect of condensation on hydrogen-air deflagrations and detonations. Both relate the effect of phase-change to instantaneous pressure peaks or valleys that appear in their experiments, without further analysis. The interesting particularities of the condensation of very hot products in narrow geometries and its potential effect on the dynamic of the flame appear to be unexplored.

This is probably due to the fact that the characteristic times of condensation are usually much longer than combustion timescales for common industrial applications. Nevertheless, for narrow gaps the experimental results show clearly that they

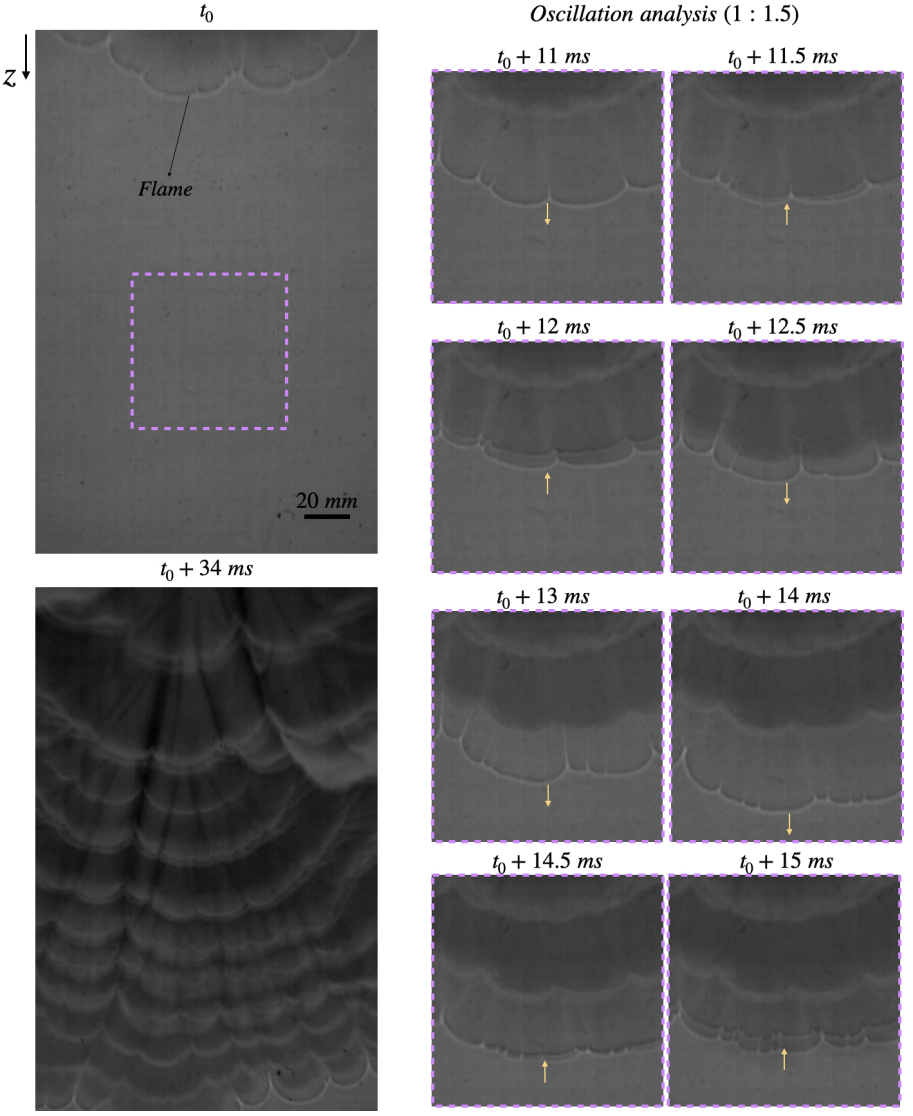

FIG. 1. *Schlieren* images of the propagation of a stoichiometric hydrogen-air flame in a channel of thickness $D = 8$ mm[1]. The flame and its local motion direction is indicated by orange arrows. The amount of water is inversely proportional to the brightness of the picture. Details with scale 1:1.5 of the dynamic of one oscillation cycle are shown on the right.

become comparable, and thus non-negligible, at these conditions.

The authors have undertaken this work encouraged by the experimental results shown before and the lack of a pertinent analytical model. Understanding of this topic should be of interest for future micro-combustor development amongst other potential applications. The main goal of this paper is to provide a theoretical interpretation of change of phase problems, which could potentially explain the described experiments.

II. THEORETICAL MODEL

A. Base model

In this paper, we endeavour the analysis of the change of phase occurring at the combustion products at a thin gap between two flat plates. Our intention is to follow a simple approach in order to achieve a very comprehensible formulation. Therefore, we initiate the analysis considering a one-dimensional problem in which two-phases are present, steam and liquid water,[17] (page 149).

Hot combustion products are generated by a flame that propagates to the left at a velocity $\dot{z}_f$ through an horizontal channel of constant thickness D. The oxidation reaction creates a zone of hot products moving to the right of the flame at a velocity U_G. Due to heat and mass exchange with the walls, the temperature of the hot gases, T_G, decreases downstream from the adiabatic flame temperature, T_b, immediately after the combustion front. Furthermore, the relatively high velocities reached by the combustion products (from the point of view of condensation), typically larger than 10 m/s, and the large void fraction, close to the unity, determine the condensation regime[17]. Condensation takes place in the so called *Annular Regime* without disperse phase. This regime is characterized by the formation of a film with dimensionless thickness α of condensed fluid on the solid walls, which are separated by a central area in which only non-condensed products exist. The analysis domain is sketched in Fig. 2.

Once the disposition of the problem has been shown, the conservation laws of mass, momentum and energy can be formulated. This should be done for each phase separately and be carried out taking into account the forces and interactions between them shown in Figs. 3 and 4. This was already brilliantly carried out by[17], equations (1)-(6).

$$\rho_L \frac{\partial(1-\alpha)}{\partial t} + \rho_L \frac{\partial(1-\alpha)U_G}{\partial z} = -\Gamma, \tag{1}$$

$$\frac{\partial \rho_G \alpha}{\partial t} + \frac{\partial \rho_G \alpha U_G}{\partial z} = \Gamma, \tag{2}$$

$$\frac{\partial \rho_L (1-\alpha) U_L}{\partial t} + \frac{\partial \rho_L (1-\alpha) U_L^2}{\partial z} + \Gamma U_I = \\ = -(1-\alpha)\frac{\partial P}{\partial z} - F_{wL} + F_I - F_{VM}, \tag{3}$$

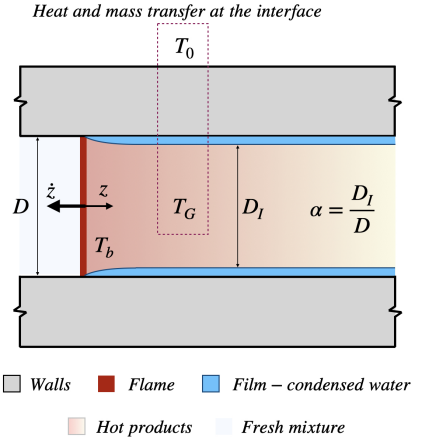

FIG. 2. Sketch of the proposed problem.

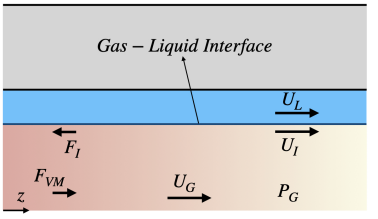

FIG. 3. Sketch of the forces in a particular section of the tube.

$$\frac{\partial \rho_G \alpha U_G}{\partial t} + \frac{\partial \rho_G \alpha U_G^2}{\partial z} - \Gamma U_I = \\ = -\alpha \frac{\partial P}{\partial z} - F_{wG} - F_I + F_{VM}, \tag{4}$$

$$\rho_L \frac{\partial\,(1-\alpha)\,(e_L - P/\rho_L)}{\partial t} + \frac{\partial \rho_L (1-\alpha) e_L U_L}{\partial z} + \Gamma e_{LI} \\ - P\frac{\partial \alpha}{\partial t} - \frac{r_L}{A}\dot{q}_w - \frac{r_I}{A}\dot{q}_{LI} - [F_I - F_{VM}]U_I = 0, \tag{5}$$

$$\frac{\partial \rho_G \alpha\,(e_G - P/\rho_G)}{\partial t} + \frac{\partial \rho_G \alpha e_G U_G}{\partial z} - \Gamma e_{GI} + P\frac{\partial \alpha}{\partial t} \\ - \frac{r_G}{A}\dot{q}_w + \frac{r_I}{A}\dot{q}_{GI} - [F_I - F_{VM}]U_I = 0. \tag{6}$$

In these expressions, the unknown variables are the amount of volume occupied by gas, α, the gas density, ρ_G, the gas velocity, U_G, the liquid velocity, U_L, the pressure, P, the liquid energy, e_L and the gas energy, e_G. Sub-index I regards

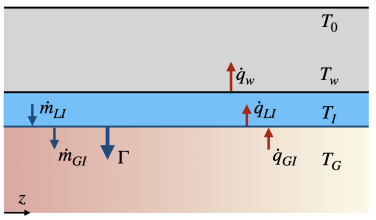

FIG. 4. Sketch of the heat and mass fluxes in a particular section of the tube.

the liquid-gas interface. Sub-Indexes *GI* and *LI* designate the fluid interface in the gaseous and liquid phase respectively. F_{wL}, F_{wG} refer to the wall forces acting in the liquid and gas respectively. F_I is the interface force. F_{VM} is the virtual mass force. $\dot{q}_w$ represent the wall heat losses. Γ is the volumetric rate of change of phase and r/A defines the different perimeter to area ratios.

Shortly summarized, in this formulation the interface between phases is the lieu where interactions between phases are accounted for. It determines most of the sources appearing in the RHS of the equations.

On those frames, the amounts of condensed water interchanged in the interface, Γ, modifies the usual continuity equation and determines the interaction between equations (1) and (2). Analogously, in impulse equations (3) and (4), a particle gets accelerated (decelerated) by the amount of mass evaporated (condensed) moving with the speed of the interface U_I. The particle further interacts due to friction with the walls and the interface itself, which velocity is determined by the two phases. On the same terms, the energy of a particle is altered in eqs. (5) and (6) by the energy of the fluid evaporated (condensed), the heat losses to the walls, the conduction or convection exchanges with the interface and the work of the friction forces.

Consequently, we sketch the interface mass and energy transfer, see Fig. 4. We follow the same formulation stated in[17] (page 157). Thus, the amount of vaporized liquid ($\dot{m} > 0$) or condensed vapour ($\dot{m} < 0$) is proportional to the difference of the heat provided from the gas to the interface minus the heat removed by the liquid,

$$h_{LG}\dot{m} = \dot{q}_{GI} - \dot{q}_{LI}. \tag{7}$$

On the one hand, we take the classic expression,

$$\dot{q}_{GI} = \dot{h}_G\,(T_G - T_I)\,, \tag{8}$$

for the heat provided by the gas, where $\dot{h}_G$ could be calculated utilizing an empirical correlation (section IV B). On the other hand, heat conduction through the liquid layer is

$$\dot{q}_{LI} = \frac{K_L}{D\,(1-\alpha)}\,(T_I - T_L)\,. \tag{9}$$

Thus,

$$\dot{m} = \frac{\dot{h}_G\,(T_G - T_I) - \dfrac{K_L}{D\,(1-\alpha)}\,(T_I - T_L)}{h_{LG}}. \tag{10}$$

Finally, the volumetric rate of change of phase, Γ, corresponds to

$$\Gamma = \dot{m} r_I / A. \tag{11}$$

We refer the readers to[17] publication for further and comprehensive details on the derivation of the formulation.

B. Simplifications

The set of equations (1)-(6) with the additional considerations (7)-(11) is quite substantial. This impedes, or at least complicates, its interpretation and the qualitative comprehension of the underlying physical phenomenon. Nevertheless, the particularities of the condensation problem of combustion products allows for significant simplifications:

1. The amount of combustion products is limited. The condensation layers forming on the surfaces remain very thin, of the order of 10 µm. Therefore, we consider that the liquid layer is in mechanical equilibrium but not in thermal one. The films do not move, but grow or decrease by condensation and evaporation. Also, they do transmit heat and change its temperature. This implies that $U_L = 0$ m/s, $U_I = 0$ m/s, $e_L \approx h_L$ and $e_{LI} \approx h_{LI}$. $U_I = 0$ m/s also means that the work of the friction force is negligible, as is mostly accepted in thermodynamics textbooks,[30].

2. The liquid-layer equilibrium hypothesis, imposes that inter-facial drag, F_I, is equal to the wall forces on the liquid layer, $F_I = F_{wL}$. Further discussion on the relative significance of friction forces is taken over below, in section II C 2, where it is more pertinent.

3. The kinetic energy of the gas ($\frac{1}{2}\rho_G U_G^2 \sim 7.5$ W with $\rho_G \approx 0.15$ kg/m^3 and $U_G \approx 10$ m/s) is negligible compared with its enthalpy at high temperature ($h_G \sim 10$ MW). Thus, $e_G \approx h_G$ and $e_{GI} \approx h_{GI}$

4. We consider a single component fluid (i.e., water and super-heated steam) in two separated phases. This can be interpreted as disregarding non-condensable components, like nitrogen. Alternatively, we can see this as if we where considering stoichiometric hydrogen-oxygen mixtures which reaction goes completely forward, disregarding equilibrium. By this, a simplified form of $\dot{h}_{GI}$ is possible.

5. Virtual Mass Force,[17] (page 162) may be important when the phases accelerate with respect to each other. This is significant only if the gas phase is dispersed. The *Annular Condensation* regime appearing in this problem precludes dispersed phases. Therefore, $F_{VM} = 0$ N.

6. We stretch the *Annular Condensation* regime to the limit and consider that the films are continuous and uninterrupted. Even if very thin, a continuous layer of liquid isolates the gas from the walls. This implies that $r_G = 0$ m and that $r_L = r_I$, thus we drop the subindexes for the perimeter. For our semi-infinite plates the perimeter area ratio is $r/A = 2/D$. Also, $F_{wG} = 0$ N.

   Considering the condensate to be a continuous film is a questionable assumption, specially when the amount of water is small, that we want to discuss in detail. Firstly, note that in equation (7) of the model of Ghiaasiaan[17] it is implicitly assumed the existence of the interface, namely, of the two phases. We apply the model consciously, even if we are aware that in our case it is possible to have conditions without any condensed water at all. Secondly, the dynamic of the condensation makes more probable that at the initial stage isolated droplets of condensed water exist. Thirdly, surface stress effects, like Marangoni forces[31], can cut the liquid film, or make the layer coalesce into droplets.

   Let us now analyze the implications of the assumption from the thermodynamic point of view. On the one hand, the amount of mass condensed is determined by the ratio between heat provided to the interface and heat evacuated to the wall. On the other hand, the temperature of the gases depends on the heat losses and on the heat of change of phase provided by the condensation. By creating a continuous film the heat losses of the gas are minimized. As $r_G = 0$ m, the gas cannot exchange directly heat with the wall. At the same time, $r_G = 0$ m, implies that the heat losses of the liquid are maximized. Results of this maximization and minimization is a simultaneous overestimation of the temperature of the gas and the condensation rate.

With all the simplifications listed above, the system of equations substantially simplifies, leading to

$$\rho_L \frac{\partial \alpha}{\partial t} = \frac{2}{D}\dot{m}, \tag{12}$$

$$\frac{\partial \rho_G \alpha}{\partial t} + \frac{\partial \rho_G \alpha U_G}{\partial z} = \frac{2}{D}\dot{m}, \tag{13}$$

$$\frac{\partial \rho_G \alpha U_G}{\partial t} + \frac{\partial \rho_G \alpha U_G^2}{\partial z} = -\alpha \frac{\partial P}{\partial z} - F_I, \tag{14}$$

$$\rho_L \frac{\partial \left(1-\alpha\right)\left(h_L - P/\rho_L\right)}{\partial t} + \Gamma h_{LI} - P\frac{\partial \alpha}{\partial t} - \\ - \frac{2}{D}\dot{q}_w - \frac{2}{D}\dot{q}_{LI} = 0, \tag{15}$$

$$\frac{\partial \rho_G \alpha \left(h_G - P/\rho_G\right)}{\partial t} + \frac{\partial \rho_G \alpha h_G U_G}{\partial z} - \Gamma h_{GI} + \\ + P\frac{\partial \alpha}{\partial t} + \frac{2}{D}\dot{q}_{GI} = 0. \tag{16}$$

C. Manipulation of the equations and further simplifications

1. Gas continuity

In equation (13) we develop the product $\frac{\partial \rho_G \alpha}{\partial t}$ and substitute equation (12) to eliminate the derivatives of α. Applying that $\rho_G \ll \rho_L$, equation (13) gets transformed into

$$\alpha \frac{\partial \rho_G}{\partial t} + \frac{\partial \rho_G \alpha U_G}{\partial z} = \frac{2}{D}\dot{m}. \tag{17}$$

2. Gas impulse

Analogously, in equation (14) we develop the product $\frac{\partial \rho_G \alpha U_G}{\partial t}$. Then, we substitute equations (12) and (17) to obtain a formulation in $\frac{\partial U_G}{\partial t}$ alone. After some simple algebra,

$$\rho_G \alpha \frac{\partial U_G}{\partial t} + \rho_G \alpha U_G \frac{\partial U_G}{\partial z} = -U_G \frac{2}{D}\dot{m} - \alpha \frac{\partial P}{\partial z} - F_I. \tag{18}$$

We now consider the results of the experiments conducted by Veiga[1]. On them, we can observe that the condensation of the reaction products is strong enough to change the propagation regime of the flame. Of course, it induces a change of shape of the combustion front, which transforms from convex to concave (Fig. 1). But most notably, it is even powerful enough to stop the flame and invert its propagation direction. We consider these interesting facts with regard to eq. (18). Left-hand side can be regarded as a *substantial derivative*. Thus, we should interpret experimental results considering right-hand sides exclusively. For slow flames, $\left|\alpha \frac{\partial P}{\partial z}\right| \ll \left|U_G \frac{2}{D}\dot{m}\right|$. Likewise, we can infer from the experiments that

$$|F_I| \ll \left|U_G \frac{2}{D}\dot{m}\right|. \tag{19}$$

The friction force should be negligible in comparison with the effect of the condensation in most regions of the products domain, as long as condensation is significant enough. Notable exceptions to this are the locations of the zeros of the $\dot{m}$ function (see section IV C), and an small ball around them. Near those locations we take

$$F_I = 2sign(U_G)\tau_w/D, \tag{20}$$

where τ_w, usually also expressed as $\tau_w = \rho_G u_\tau^2$, is the stress at the wall. The calculation of this magnitude is a classic topic of boundary layer theory. For the conditions of interest, $u^+ = y^+$. Thus, considering $y = D/2$, then $U_G = D u_\tau^2/(2\nu)$ where ν is the kinematic viscosity. For further discussion, we refer to[32].

At the conditions of interest (see section VI A), an order of magnitude analysis of both friction and condensation gives for $U_G \approx 10$ m/s, $|\dot{m}| \approx 0.1$ kg/m^2/s, $\rho_G \approx 0.15$ kg/m^3, a characteristic friction factor $f_I \approx 0.005$,[17], and $D \approx 0.01$ m, $F_I =$

$2\tau_I/D = \rho_G U_G^2 f_I/D \sim 7.5$. At the same time, $2U_G|\dot{m}|/D \sim 200$. Thus $F_I \ll 2U_G|\dot{m}|/D$ can be considered when relatively slow flames –which determines the velocity of the combustion products– propagate through narrow geometries with high-enough condensation/vaporization rate.

3. Energy of the liquid

Turning again to the partial derivatives, we develop the product

$$\rho_L \frac{\partial\,(1-\alpha)\,(h_L - P/\rho_L)}{\partial t} = \rho_L\,(1-\alpha)\,\frac{\partial}{\partial t}\,(h_L - P/\rho_L) - \rho_L\,(h_L - p/\rho_L)\,\frac{2}{D}\frac{\dot{m}}{\rho_L}. \quad (21)$$

We substitute the last equation and equation (9) into equation (15). After some simplifications,

$$\rho_L\,(1-\alpha)\,\frac{\partial}{\partial t}\left(h_L - \frac{P}{\rho_L}\right) + \frac{2}{D}\dot{m}\,(h_{LI} - h_L) - - \frac{2\dot{q}_w}{D} - \frac{2K_L}{D^2\,(1-\alpha)}\,(T_I - T_L) = 0. \quad (22)$$

4. Energy of the gas

We will develop the products inside of the two first differentials in equation (16). After substituting equations (12) and (17), the first derivative is

$$\frac{\partial \rho_G \alpha\,(h_G - P/\rho_G)}{\partial t} = = \left(h_G - \frac{P}{\rho_G}\right)\left[-\frac{\partial \rho_G \alpha U_G}{\partial z} + \frac{2}{D}\dot{m}\right] + + \rho_G \alpha \frac{\partial\,(h_G - P/\rho_G)}{\partial t}. \quad (23)$$

We also have,

$$\frac{\partial \rho_G \alpha h_G U_G}{\partial z} = h_G \frac{\partial \rho_G \alpha U_G}{\partial z} + \rho_G \alpha U_G \frac{\partial h_G}{\partial z} \quad (24)$$

Substituting equations (23) and (24) in (16) and applying once again that $\rho_G \ll \rho_L$,

$$\rho_G \alpha \frac{\partial\,(h_G - P/\rho_G)}{\partial t} + \frac{2}{D}\dot{m}\,(h_G - h_{GI}) - \frac{2}{D}\dot{m}\frac{P}{\rho_G} + + \frac{P}{\rho_G}\frac{\partial \rho_G \alpha U_G}{\partial z} + \rho_G \alpha U_G \frac{\partial h_G}{\partial z} + \frac{2}{D}\dot{h}_G\,(T_G - T_I) = 0. \quad (25)$$

5. Recapitulation

With the transformations of the previous sections, the system of equations that obtained until now is,

$$\frac{\partial \alpha}{\partial t} = \frac{2}{D}\frac{\dot{m}}{\rho_L}, \quad (26)$$

$$\alpha \frac{\partial \rho_G}{\partial t} + \frac{\partial \rho_G \alpha U_G}{\partial z} = \frac{2}{D}\dot{m}, \quad (27)$$

$$\rho_G \alpha \frac{\partial U_G}{\partial t} + \rho_G \alpha U_G \frac{\partial U_G}{\partial z} = -U_G \frac{2}{D}\dot{m} - \alpha \frac{\partial P}{\partial z}, \quad (28)$$

$$\rho_L\,(1-\alpha)\,\frac{\partial}{\partial z}\left(h_L - \frac{P}{\rho_L}\right) + \frac{2}{D}\dot{m}\,(h_{LI} - h_L) - - \frac{2}{D}\dot{q}_w - \frac{2K_L}{D^2\,(1-\alpha)}\,(T_I - T_L) = 0, \quad (29)$$

$$\rho_G \alpha \frac{\partial\,(h_G - P/\rho_G)}{\partial t} + \frac{2}{D}\dot{m}\,(h_G - h_{GI}) - \frac{2}{D}\dot{m}\frac{P}{\rho_G} + + \frac{P}{\rho_G}\frac{\partial \rho_G \alpha U_G}{\partial z} + \rho_G \alpha U_G \frac{\partial h_G}{\partial z} + \frac{2}{D}\dot{h}_G\,(T_G - T_I) = 0. \quad (30)$$

III. ASYMPTOTIC EXPANSION CONSIDERING A THIN LIQUID LAYER. TEMPERATURE OF THE LIQUID

It was already discussed in section II B that liquid layers appearing on the walls of the combustion chamber remain forcibly very thin. This suggests performing an asymptotic expansion ([33]) considering that $(1-\alpha) \to 0$. This term appears in eq. (29) and (10). Let us consider these equations in detail.

A. Enthalpy of the liquid equation. Initial approximation

Let us call $(1-\alpha) = \varepsilon$, a small parameter. We now write $h_L \approx cT_L$ and expand the pressure and the temperature as follows,

$$T_L = T_{L0} + T_{L1}\varepsilon, \quad (31)$$

$$P_L = P_{L0} + P_{L1}\varepsilon. \quad (32)$$

We develop eq. (29) in terms of ε, getting

$$\rho_L \varepsilon^2 \frac{\partial}{\partial t}\left(c\,(T_{L0} + T_{L1}\varepsilon) - \frac{P_{L0} + P_{L1}\varepsilon}{\rho_L}\right) + + \varepsilon \frac{2}{D}\dot{m}c\,(T_I - T_{L0} - T_{L1}\varepsilon) - - \frac{2}{D}\dot{q}_w\varepsilon - \frac{2K_L}{D^2}\,(T_I - T_{L0} - T_{L1}\varepsilon) = 0. \quad (33)$$

In zero order, this means

$$T_I = T_{L0}, \quad (34)$$

whilst in first order

$$\frac{2}{D}\dot{m}c\,(T_I - T_{L0}) - \frac{2}{D}\dot{q}_w + \frac{2K_L}{D^2}T_{L1} = 0. \quad (35)$$

So,

$$T_{L1} = \frac{D\dot{q}_w}{K_L}. \quad (36)$$

Grouping terms,

$$T_L = T_I + \frac{D\dot{q}_w}{K_L}\,(1-\alpha). \quad (37)$$

B. $\dot{m}$ development

Equation (37) constitutes a generic result considering $\dot{m}$ of zero order. Now, we also include in the analysis the expansion of $\dot{m}$,

$$\dot{m} = \frac{\dot{h}_G\left(T_{G0} + T_{G1}\varepsilon - T_I\right) - \dfrac{K_L}{D\varepsilon}\left(T_I - T_{L0} - T_{L1}\varepsilon\right)}{h_{LG}}, \quad (38)$$

or equivalently,

$$\dot{m} = \frac{1}{\varepsilon}\left[-\frac{K_L}{Dh_{LG}}\left(T_I - T_{L0}\right)\right] + \\ + \frac{\dot{h}_G\left(T_{G0} - T_I\right) + K_L T_{L1}/D}{h_{LG}}. \quad (39)$$

Let us now develop the product, substituing $\dot{m}$,

$$\varepsilon c\dot{m}\left(T_I - T_{L0} - T_{L1}\varepsilon\right) = \left(-\frac{K_L c}{Dh_{LG}}\left(T_I - T_{L0}\right) + \right. \\ \left. + \frac{\varepsilon c}{h_{LG}}\left[\dot{h}_G\left(T_{G0} - T_I\right) + \frac{K_L}{D}T_{L1}\right]\right) \cdot \\ \cdot \left(T_I - T_{L0} - T_{L1}\varepsilon\right) \approx$$

$$\approx -\frac{K_L c}{Dh_{LG}}\left(T_I - T_{L0}\right)^2 + \frac{K_L c}{Dh_{LG}}\left(T_I - T_{L0}\right)T_{L1}\varepsilon + \\ + \frac{c}{h_{LG}}\left[\dot{h}_G\left(T_{G0} - T_I\right) + \frac{K_L}{D}T_{L1}\right]\left(T_I - T_{L0}\right)\varepsilon \quad (40)$$

We substitute this expression in eq. (33). In order zero, it yields,

$$-\frac{2}{D}\frac{K_L c}{Dh_{LG}}\left(T_I - T_{L0}\right)^2 - \frac{2}{D}\frac{K_L}{D}\left(T_I - T_{L0}\right) = 0. \quad (41)$$

Thus, we obtain two solutions. The first one,

$$T_I - T_{L0} = -h_{LG}/c, \quad (42)$$

has no physical sense. The second,

$$T_I = T_{L0}, \quad (43)$$

is the same as before. Now we address the result in order one. It yields,

$$\frac{K_L c}{Dh_{LG}}\left(T_I - T_{L0}\right)T_{L1} + \\ + \frac{c}{h_{LG}}\left[\dot{h}_G\left(T_{G0} - T_I\right) + \frac{K_L}{D}T_{L1}\right]\left(T_I - T_{L0}\right) \\ - \frac{2}{D}\dot{q}_w + \frac{2K_L}{D^2}T_{L1} = 0. \quad (44)$$

We apply here the already available result of eq. (43). The two first terms cancel. Therefore,

$$T_{L1} = \frac{D}{K_L}\dot{q}_w. \quad (45)$$

And we finally obtain the same result of equation (37),

$$T_L = T_I + \frac{D\dot{q}_w}{K_L}\left(1 - \alpha\right). \quad (46)$$

IV. AMOUNT OF STEAM CONDENSED

We substitute formula (46) in equation (10). It yields

$$\dot{m} = \frac{\dot{h}_G\left(T_G - T_I\right) + \dot{q}_w}{h_{LG}}. \quad (47)$$

This result states that, up to second order, the heat accumulated in the liquid layer is irrelevant for vaporization and condensation. At the same time, we observe that the heat loss to the wall is a very significant magnitude. Thus, we need to provide an expression for $\dot{q}_w$. We would do that based in different hypothesis.

A. Heat losses to the wall

1. *Thin plate hypothesis*

Let us suppose that the solid material of the plates is very thin. Under such circumstances, it is reasonable to consider

$$\dot{q}_w \approx -\frac{K_M}{e}\left(T_L - T_0\right). \quad (48)$$

Where K_M is the heat conductivity in the metal, e is the thickness of the plate and T_0 is the temperature of the plate in the exterior. Introducing the result of the liquid temperature, eq. (46), into equation (48), we reach

$$\dot{q}_w = -\frac{\dfrac{K_M}{e}\left(T_I - T_0\right)}{1 + \dfrac{K_M}{K_L}\dfrac{D}{e}\left(1 - \alpha\right)}. \quad (49)$$

Using the fact that $(1-\alpha) \to 0$, we Taylor expand, and introduce the results in eq. (47). Thus obtaining

$$\dot{m} = \frac{\dot{h}_G\left(T_G - T_I\right)}{h_{LG}} - \\ - \frac{k_M}{eh_{LG}}\left(T_I - T_0\right)\left[1 + \frac{K_M}{K_L}\frac{D}{e}\left(1 - \alpha\right)\right]. \quad (50)$$

In zero order, this simplifies to

$$\dot{m} \approx \frac{\dot{h}_G\left(T_G - T_I\right) - \dfrac{k_M}{e}\left(T_I - T_0\right)}{h_{LG}}. \quad (51)$$

2. *Semi-infinite plate hypothesis*

We suppose now that the thickness of the plate is semi infinite. For such configuration the temperature distribution and the heat transfer are well known. Following[34],

$$\frac{T - T_L}{T_L - T_0} = erf\left(\eta\right). \quad (52)$$

In the previous expression, erf is the error function, $\eta = z/\sqrt{4\pi\alpha_M t}$ and $\alpha_M = K_M/(\rho_M c_M)$. We will derive the magnitude of interest, $\dot{q}_w = -K_M \left.\frac{\partial T}{\partial z}\right|_0$, from it. It is easy to see that,

$$\dot{q}_w = -\frac{K_M (T_L - T_0)}{\sqrt{\pi\alpha_M t}}. \tag{53}$$

We substitute the last result into formula (46) to get

$$\dot{q}_w = \frac{-\frac{K_M}{\sqrt{\pi\alpha_M t}}(T_I - T_0)}{1 + \frac{K_M}{\sqrt{\pi\alpha_M t}}\frac{D}{K_L}(1-\alpha)}. \tag{54}$$

We Taylor expand the last expression utilizing $(1-\alpha) \to 0$, and introduce this result in eq. (47). It yields

$$\dot{m} = \frac{\dot{h}_G (T_G - T_I)}{h_{LG}} - \\ - \frac{K_M}{\sqrt{\pi\alpha_M t}}\frac{(T_I - T_0)}{h_{LG}}\left[1 - \frac{K_M}{\sqrt{\pi\alpha_M t}}\frac{D}{K_L}(1-\alpha)\right]. \tag{55}$$

Which in zero order provides

$$\dot{m} \approx \frac{\dot{h}_G (T_G - T_I) - \frac{K_M}{\sqrt{\pi\alpha_M t}}(T_I - T_0)}{h_{LG}}. \tag{56}$$

The formulae above depend on the time, t, elapsed since the combustion front have heated for the first time a certain location z of the channel. We may reformulate equation (56) in order to exclude that time. We do that considering a quasi-steady state in which the flame moves with a constant speed of module $|\dot{z}_f|$ towards the left of the domain. In these conditions, $t = \left(z - z_f(t)\right)/|\dot{z}_f|$, leading to

$$\dot{m} \approx \frac{\dot{h}_G (T_G - T_I) - \frac{K_M\sqrt{|\dot{z}_f|}}{\sqrt{\pi\alpha_M\left(z - z_f(t)\right)}}(T_I - T_0)}{h_{LG}}. \tag{57}$$

By analogy with the $\dot{h}_G$ formulation, we denote

$$\dot{h}_w = \frac{K_M\sqrt{|\dot{z}_f|}}{\sqrt{\pi\alpha_M\left(z - z_f(t)\right)}} = \sqrt{\frac{K_M\rho_M c_M \dot{z}_f}{\pi\left(z - z_f(t)\right)}}. \tag{58}$$

We finalize this section with a small caveat. It is the opinion of the authors that both assumptions of *thin wall* or *semi-infinite wall* should be unsatisfactory when applied to walls build with high-conductive materials like metals. A refined assumption on the heat transmission to the wall should be adopted in that case.

B. Convective heat transfer to a flat layer

1. Area close enough to the reactive region

For an area close enough to the flame, the flow configuration is analogous to the well-known semi-infinite flow over a flat plate. From[34], the local Nusselt number, at a distance z downstream from the edge of the plate, is given by

$$Nu = 0.332 Re_z^{1/2} Pr^{1/3}. \tag{59}$$

Evidently, the *edge* to be considered is the flame. Therefore we have $Nu = \dot{h}_G\left(z - z_f(t)\right)/k_G$ and $Re_z = \left(z - z_f(t)\right)U_G/\nu_G$. Thus,

$$\dot{h}_G = 0.332 K_G \sqrt{\frac{U_G}{\left(z - z_f(t)\right)\nu_G}} Pr^{1/3}. \tag{60}$$

2. General convective heat transfer equation considered

After a thorough review of heat transfer documentation,[34–38] among others, it was found that several formulations with different degrees of approximation are available to reproduce heat transfer by convection in between plates.

For our study, it is of critical importance the behavior of the expressions at the region close to the flame, where the thermal boundary layer is still developing and most of the heat transfer takes place. However, most of correlations do not show the $z^{-1/2}$ dependence that should appear at the flame region (see discussion in section V C for justification of this assessment).

Finally, the correlation developed by Stephan[39] was selected for the case at hand. It provides the Nusselt number that characterizes convective heat transfer,

$$Nu_z = 7.55 + \frac{0.024(z^*)^{-1.14}}{1 + 0.0358 Pr^{0.17}(z^*)^{-0.64}}, \tag{61}$$

where $z^* = z/\left(D_h Re_{D_h} Pr\right)$ and $D_h = 2D$ is the hydraulic diameter of two flat parallel plates. Therefore,

$$\dot{h}_G = \frac{Nu_z K_G}{z - z_f(t)}. \tag{62}$$

This expression takes the approximate form of formula (60) when $z \to 0$.

C. Analysis of the zeros of $\dot{m}$

For the simplicity of the formulation, we will perform the following analysis making use of equation (60). Therefore the results are only strictly valid close to the flame. However, similar results are expected to appear if we use eq. (62) but with different correlation constants.

1. Thin layer approach

We return to equation (51), which provided $\dot{m}$ in zero order. Substituting equation (60) in it,

$$\dot{m} = 0.332 K_G \sqrt{\frac{U_G}{(z-z_f)\nu_G}} Pr^{1/3} \frac{(T_G - T_I)}{h_{LG}} - \\ - \frac{K_M}{e h_{LG}} (T_I - T_0) . \tag{63}$$

A priori, this equation exhibit a single zero. With $z \to \infty$ the first term always decreases with distance. A second zero is obtained for $z \to \infty$, also $P \to 0$, but much earlier, $T_I \to T_0$. This is a depression that reduces second term of RHS to zero the whole function. An unsatisfactory dynamic, considering the real processes.

2. Semi-infinite solid approach

We substitute equation (60) in (56). It yields,

$$\dot{m} = 0.332 K_G \sqrt{\frac{U_G}{(z-z_f)\nu_G}} Pr^{1/3} \frac{(T_G - T_I)}{h_{LG}} - \\ - \sqrt{\frac{\rho_M c_M K_M}{\pi t}} \frac{(T_I - T_0)}{h_{LG}} . \tag{64}$$

We are explicitly avoiding to utilize the previously derived quasi-stationary formulation. We call,

$$K^* = 0.332 K_G Pr^{1/3} \sqrt{\frac{\pi}{\rho_M c_M K_M \nu_G}} . \tag{65}$$

Looking for the zeros and reordering, the much more complex solution,

$$K^* \sqrt{\frac{U_G t}{z-z_f}} (T_G - T_I) = (T_I - T_0) , \tag{66}$$

is derived. Now, let us rewrite the distance from the flame as,

$$z - z_f = \int \dot{z}_f dt . \tag{67}$$

Therefore,

$$K^* \sqrt{\frac{U_G}{\frac{1}{t}\int \dot{z}_f dt}} (T_G - T_I) = (T_I - T_0) . \tag{68}$$

But of course,

$$\overline{\dot{z}_f} = \frac{1}{t} \int \dot{z}_f dt . \tag{69}$$

So that,

$$K^* \sqrt{\frac{U_G}{\overline{\dot{z}_f}}} = \frac{T_I - T_0}{T_G - T_I} . \tag{70}$$

This last equation represents a rich dynamic, in which perturbations among the fluid motion, the flame propagation or the temperature of the gas can generate multiple zeros. We consider U_G, T_G the conditions of a zero for $\dot{m}$. Introducing a small perturbation δ in the variables,

$$K^* \sqrt{\frac{U_G + \delta_{U_G}}{\overline{\dot{z}_f}}} = \frac{T_I - T_0}{T_G + \delta_{T_G} - T_I} . \tag{71}$$

It simplifies to

$$\frac{\delta_{U_G}}{2U_G} = \frac{\delta_{T_G}}{T_G - T_I} , \tag{72}$$

leading to an infinity of solutions that depend on the combination of the values of the gas velocity, its temperature and their corresponding perturbations. Thus we conclude that the existence of an infinity of zeros of $\dot{m}$ depends on the assumption considered to treat the thickness of wall, but not on wall characteristics, subsumed in variable K^*, that is not present in eq. (72). The notable difference of behavior between thin and thick tubes can be observed comparing eqs. (63) and (64). The existence of zeroes for thick walls is related to the *transient* behavior of heat transfer. The infinitely thin tubes do not reflect the progressive heating of the wall, disregarding the progressive non-linear heat penetration inside of the solid, as well as the asymptotic character of the solution at $t \to 0$ s.

V. ZERO ORDER SYSTEM OF EQUATIONS

A. Laboratory coordinates

We consider again the system (26)-(30) under the thin liquid layer hypothesis and asymptotic expansion. We note that very important simplifications have been achieved. Equation (26) is no longer necessary. The same as equation (29), because T_L has been expressed through the asymptotic analysis. We need to carry out the asymptotic development of equations (27), (28) and (30). But this, to zero order, is immediate, as α appears isolated, and no $(1-\alpha)$ group exist in those equations. The amount of mass condensed, $\dot{m}$, was a term of order -1. Nevertheless, the developments of section IV has allowed to express this variable as a zero order magnitude. This simplifies significantly the asymptotic expansion. Summarizing,

$$\begin{pmatrix} 1 & 0 & 0 \\ 0 & \rho_G & 0 \\ 0 & 0 & \rho_G \end{pmatrix} \begin{pmatrix} \frac{\partial \rho_G}{\partial t} \\ \frac{\partial U_G}{\partial t} \\ \frac{\partial \varepsilon_G}{\partial t} \end{pmatrix} + \\ + \begin{pmatrix} U_G & \rho_G & 0 \\ 0 & \rho_G U_G & 0 \\ \frac{P}{\rho_G} U_G & P & \rho_G U_G \end{pmatrix} \begin{pmatrix} \frac{\partial \rho_G}{\partial z} \\ \frac{\partial U_G}{\partial z} \\ \frac{\partial h_G}{\partial z} \end{pmatrix} + \begin{pmatrix} 0 \\ \frac{\partial P}{\partial z} \\ 0 \end{pmatrix} =$$

$$= \frac{2\dot{m}}{D}\begin{pmatrix}1\\ -U_G\\ -(\varepsilon_G - h_{GI})\end{pmatrix} - \frac{2}{D}\begin{pmatrix}0\\ 0\\ \dot{h}_G(T_G - T_I)\end{pmatrix} - \\ - \frac{2}{D}\begin{pmatrix}0\\ sign(U_G)\tau_w\\ 0\end{pmatrix}. \quad (73)$$

This system together with formulae (61) and (51) or (56) make a closed system.

We may now examine equation (73). The left hand side corresponds to the usual convective terms and gradient of pressure. The right hand sides comprises more interesting terms. The first is a source/sink of mass, with its corresponding effect in the gas impulse and the heat losses. Note that when condensation takes places, $\dot{m} < 0$, ρ_G *decreases*, and the heat provided by the change of phase increases the gas temperature. *But note also that the flow accelerates*. The second term corresponds just to heat losses to the static liquid layer. The third term is a sink of momentum due to friction forces.

Despite its size, equation (73) simply states that a particle of gas is decelerated by the gradient of pressure and the friction force, and accelerated by the depression created by condensation. It also asserts that the hot particle heats the wall and gets heated by its own condensation.

B. Change of coordinates. Axis attached to the flame

We consider now the axis of reference z attached to the flame. We conveniently set that it travels to the left, leading to negative propagation velocities, $\dot{z}_f < 0$. Following[40], we carry out the change of coordinates,

$$\zeta = z - z_f(t), \quad (74)$$
$$\tau = t. \quad (75)$$

For the derivatives it results into,

$$\frac{\partial}{\partial t} = \frac{\partial}{\partial \tau} - \dot{z}_f \frac{\partial}{\partial \zeta}, \quad (76)$$
$$\frac{\partial}{\partial z} = \frac{\partial}{\partial \zeta}. \quad (77)$$

We rewrite equation (73) into these coordinates. We also express it in terms of internal energy, and invert the first matrix. It yields,

$$\begin{pmatrix}\frac{\partial \rho_G}{\partial \tau}\\ \frac{\partial U_G}{\partial \tau}\\ \frac{\partial \varepsilon_G}{\partial \tau}\end{pmatrix} + \left(\begin{pmatrix}U_G & \rho_G & 0\\ 0 & U_G & 0\\ 0 & \frac{P}{\rho_G} & U_G\end{pmatrix} - \dot{z}_f I\right)\begin{pmatrix}\frac{\partial \rho_G}{\partial \zeta}\\ \frac{\partial U_G}{\partial \zeta}\\ \frac{\partial \varepsilon_G}{\partial \zeta}\end{pmatrix} + \\ + \begin{pmatrix}0\\ \frac{1}{\rho_G}\frac{\partial P}{\partial \zeta}\\ \frac{U_G}{\rho_G}\frac{\partial P}{\partial \zeta}\end{pmatrix} = \frac{2\dot{m}}{D\rho_G}\begin{pmatrix}\rho_G\\ -U_G\\ -(\varepsilon_G - h_{GI})\end{pmatrix} - \\ - \frac{2}{D\rho_G}\begin{pmatrix}0\\ 0\\ \dot{h}_G(T_G - T_I)\end{pmatrix} - \frac{2}{D\rho_G}\begin{pmatrix}0\\ sign(U_G)\tau_w\\ 0\end{pmatrix}. \quad (78)$$

We can now define very simply the boundary conditions in the left limits of the calculation domain. Those are the ones of the products of combustion in a location immediately after the flame,

$$\rho_G|_0 = \rho_b, \quad (79)$$
$$u_G|_0 = -\dot{z}_f(\sigma - 1), \quad (80)$$
$$\varepsilon_G|_0 = \varepsilon_b, \quad (81)$$

being σ the expansion factor.

C. Dimensional analysis

1. General

For convenience for the rest of the analysis we rewrite the mass condensation as,

$$\dot{m} = \frac{\dot{h}_G}{h_{LG}}(T_G - T_I)\left[1 - \frac{\dot{h}_w}{\dot{h}_G}\frac{T_I - T_0}{T_G - T_I}\right]. \quad (82)$$

Subsequently, we take S_L, D, ρ_0, T_{G0} as dimensional magnitudes. We also utilize the equality $\tau_w = \rho_G u_\tau^2$ for the boundary layer. The construction of the dimensionless equations is carried out utilizing these magnitudes and equation (78). We utilize S_L^2 for the scaling of the energetic magnitudes. After a tedious but uncomplicated algebra,

$$\begin{pmatrix}\frac{\partial \rho_G}{\partial \tau}\\ \frac{\partial U_G}{\partial \tau}\\ \frac{\partial \varepsilon_G}{\partial \tau}\end{pmatrix} + \left(\begin{pmatrix}U_G & \rho_G & 0\\ 0 & U_G & 0\\ 0 & \frac{P}{\rho_G} & U_G\end{pmatrix} - \dot{z}_f I\right)\begin{pmatrix}\frac{\partial \rho_G}{\partial \zeta}\\ \frac{\partial U_G}{\partial \zeta}\\ \frac{\partial \varepsilon_G}{\partial \zeta}\end{pmatrix} + \\ + \begin{pmatrix}0\\ \frac{1}{\rho_G}\frac{\partial P}{\partial \zeta}\\ \frac{U_G}{\rho_G}\frac{\partial P}{\partial \zeta}\end{pmatrix} = -2\begin{pmatrix}0\\ sgn(U_G)u_\tau^2\\ 0\end{pmatrix} + \frac{\dot{h}_G T_{G0}}{\rho_0 S_L^3}\frac{2(T_G - T_I)}{\rho_G} \cdot \\ \cdot \left[\frac{1}{h_{LG}}\begin{pmatrix}\rho_G\\ -U_G\\ -(\varepsilon_G - h_{GI})\end{pmatrix}\left[1 - \frac{\dot{h}_w}{\dot{h}_G}\frac{T_I - T_0}{T_G - T_I}\right] - \begin{pmatrix}0\\ 0\\ 1\end{pmatrix}\right] \quad (83)$$

With just two dimensionless groups,

$$\frac{\dot{h}_G T_{G0}}{\rho_0 S_L^3},\ \left[1-\frac{\dot{h}_w}{\dot{h}_G}\frac{T_I-T_0}{T_G-T_I}\right] \tag{84}$$

2. Conditions for condensation immediately after the flame

Observing these groups a new condition on the nature of $\dot{h}_w$ and $\dot{h}_G$ appear. To prevent an infinite vaporization or condensation when $z\to 0$ the order of z in $\dot{h}_w$ and $\dot{h}_G$ must be the same. This pose a serious restriction on the correlations that are adequate for the calculation of $\dot{h}_G$. Remember that very numerous correlations and approximations exist for this magnitude in literature, but only those with dependence $z^{-1/2}$ when $z\to 0$ are acceptable.

We utilize the formulations $\dot{h}_w$ and $\dot{h}_G$ of equations (58) and (60). In a close environment of the beginning of the flat layer, the heat losses are analogous to the ones of a flat plate. Taking the limit,

$$\lim_{z\to 0}\frac{\dot{h}_w}{\dot{h}_G}\frac{T_I-T_0}{T_G-T_I} = \\ = \frac{3}{\sqrt{\pi}}\sqrt{\frac{K_M}{K_G}\frac{\rho_M c_M}{\rho_G c_G}}Pr_G^{1/6}\sqrt{\frac{1}{\sigma-1}}\frac{T_I-T_0}{T_G-T_I}. \tag{85}$$

Thus, the sign of the dimensionless difference,

$$1-\frac{3}{\sqrt{\pi}}\frac{K_M}{K_G}\sqrt{\frac{\alpha_G}{\alpha_M}}Pr_G^{1/6}\sqrt{\frac{1}{\sigma-1}}\frac{T_I-T_0}{T_G-T_I}, \tag{86}$$

determines whether the condensation starts immediately after the flame or not.

VI. RESULTS AND DISCUSSION

After the theoretical developments of the previous sections we perform here some numerical experiments.

A. Conditions of the numerical analysis

Equation (78) together with the boundary conditions given in (79)-(81), describe the behaviour of the combustion products inside the domain of interest. Pitifully, they depend on an unknown parameter, the laminar burning velocity.

This magnitude is related to the conditions at the extremes of the plates. Its value might be calculated integrating the flow equations throughout the whole space between the plates, including reactants and products. The pertinent boundary conditions at the borders of the plate are then applied. As far as we understand it, that was the methodology followed by[40–46].

A similar approach in our case is nevertheless impossible. In its actual formulation, the model described in this paper only applies to the products, preventing the extension of the integrals to the whole domain of a combustion problem.

Clearly, the inherent three dimensional flame dynamics cannot be expressed in 1-D. Notably, for flames propagating in slender geometries, such as the narrow gap between two plates or chambers with a large aspect ratio, wall friction[47], viscous effects in the vicinity of the wall[48], gas compression[49], thermal expansion and obstacles[50] becomes crucial processes. All of them as well as the topology, shape and size of the flame front[51] are of a 3D or, at least, 2D nature.

Therefore, at this stage of the investigation, we restrict ourselves to integrate equation (78) in stationary conditions. Thus, $\dot{z}_f$ should be considered a parameter. Note that our construct is applicable to dynamic calculations. It should be coupled with a 2D or 3D model describing the dynamic of the flame.

Under such circumstances, the boundary conditions of equations (79)-(81), imposed on the left border of calculation domain, suffice for the integration.

The numerical integration is carried out utilizing a finite differences scheme written on an in-house *Python* code. As calculations are one dimensional, resolution does not constitute an issue. Thus, it was raised at will to verify the convergence of solution. A real gases model was utilized for the calculation of enthalpies, internal energies, as well as parameters relevant to the change of phase. This was carried out using the *Cantera* library[52].

The boundary conditions were calculated as follows. Firstly, a stoichimetric hydrogen-oxygen mixture at a temperature and pressure T_{mix}, P_{mix} are loaded into *Cantera*. Subsequently, chemical equilibrium is imposed. The expansion factor, σ, is so calculated. The conditions of the products we are going to impose are not those of equilibrium. We seek for similar conditions but considering just pure steam. From the expansion factor we derive the temperature $T_G|_{z=0} = \sigma T_{mix}$, the velocity $u_G|_{z=0} = -\dot{z}_f(\sigma-1)$ and the pressure, $P = P_{mix} + \rho_{mix}u_G^2/\sigma$, immediately after the flame.

B. Base case

We consider a nominal *base case* that will help with the comparisons in parametric studies. Its conditions are enumerated below:

The gap between plates is $D = 10$mm. The fresh mixture has a temperature $T_{mix} = 300\,\mathrm{K}$ and a pressure $P_{mix} = 100\,\mathrm{kPa}$. The flame propagates at a constant velocity of $\dot{z}_f = -2.4\,\mathrm{m\,s^{-1}}$ (to the left). The density of water is $\rho_L = 1000\,\mathrm{kg\,m^{-3}}$.

As in the experiments, we consider the combustion chamber conformed of *Plexiglas* plates, with characteristics $K_M = 0.185\,\mathrm{MW\,m^{-1}\,K^{-1}}$, $\rho_M = 1180\,\mathrm{kg\,m^{-3}}$ and $c_M = 1400\,\mathrm{J\,kg^{-1}\,K^{-1}}$.

C. Variable gap thickness D

For the first parametric study, we consider five thicknesses of the gap between two parallel plates: $D =$ 2.5, 5, 7.5, 10, 25 mm. We begin studying the results for the three mechanisms that control the problem at hand. These

are the heat exchange from the gas to the walls $\dot{q} > 0$, the heat losses through the walls $\dot{q} < 0$ (Fig. 5) and the amount of condensed water $\dot{m}$ (Fig. 6). The later is related to the previous functions by equation (47).

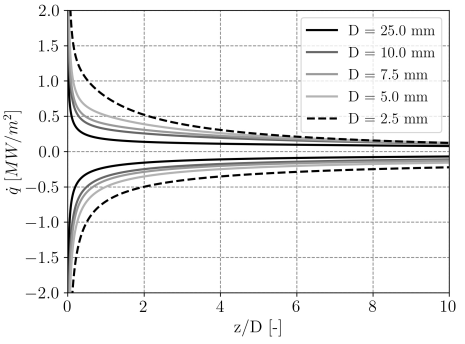

FIG. 5. Heat fluxes. Positive values represent $\dot{q}_{GI}$, negative ones refer to $\dot{q}_w$.

The first notable result is the extremely high amount of heat exchanged at the interface at regions very close to the flame, which progressively decreases when moving away from it. This behaviour appears because $\dot{q} \to \infty$ when $z \to 0$, and relaxes for higher values of z. This can be verified in eq. (62) for the gases and eq. (58) for the solid.

Reducing the channel thickness, the volume-to-area ratio increases and, therefore, the heat exchange rate rises dramatically, observing differences at $z/D = 2$ of around 80% between $D = 10$ mm and $D = 2.5$ mm.

The difference between the represented heat fluxes provides the amount of condensed ($\dot{m} < 0$) or vaporized ($\dot{m} > 0$) water, which is shown in Fig. 6. We observe intense condensation immediately behind the flame, followed by an evaporation area. An increase in the distance between the plates, enlarge the vaporization area but reduces its rate.

Further downstream, condensation occurs again before the limit $z/D = 10$ is reached. It happens though at much lower rates than those close to the flame. Note that we already studied theoretically the existence of condensation immediately after the flame in section V C. Depending on the particular material of the solid walls and the composition of the gas, evaporation (provided that some water is already existing on the walls) can also happen.

The explained behaviour can also be related to the zebra-like patterns shown in Fig. 1. Limitations in the model, supposedly due to stationary flame propagation, prevent us to see a more complex, cyclic condensation pattern. However, these results are very promising at this early stage of the investigation.

A combination of the heat and mass fluxes depicted above and the stealthy presence of friction, will determine the thermodynamic conditions and the velocity of the gaseous phase.

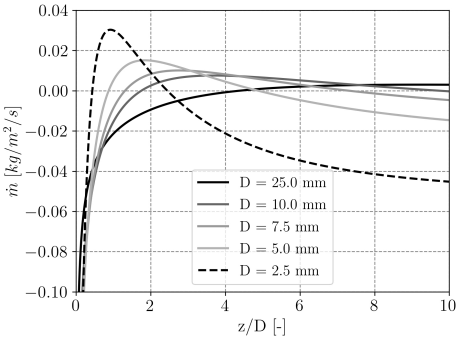

FIG. 6. Amount of vaporized liquid ($\dot{m} > 0$) or condensed vapour ($\dot{m} < 0$) at the chosen domain calculated for five gap thicknesses.

Firstly, the temperature (Fig. 7) decreases monotonically. From the adiabatic flame temperature T_b right behind the flame it progressively reaches colder values. When the vapour (liquid) condensates (evaporates), this exothermic (endothermic) procedure locally increases (decreases) the temperature of a particular section.

The quick change in gas temperature close to the front is due to the extreme heat losses that appear behind the flame. Furthermore, thin channels will suffer stronger losses, thus cooling faster. At the same time, the exchange of mass between the liquid and gaseous phase modifies locally, and not in a negligible way, these variables.

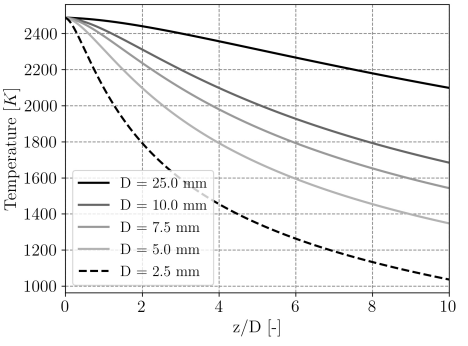

FIG. 7. Temperature of the gaseous products calculated for five gap thicknesses.

In particular, such strong heat losses and subsequent decrease of the gas temperature lead to an increase of gas density (Fig. 8), regardless of condensed mass. Influence of gas layer thickness is similar but opposite to the trends shown for temperature. The thinner the channel the higher the final den-

sity of the gaseous phase is. This can be directly related to the much lower temperatures obtained for thinner channels. Regarding the pressure, only variations of the order of Pascals are recorded and, therefore, we can consider the process to be quasi-isobaric.

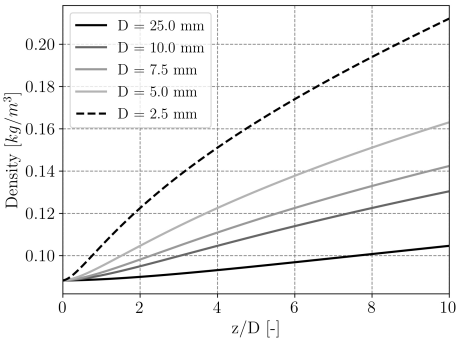

FIG. 8. Density of the gaseous products calculated for five gap thicknesses.

The combination of the thermodynamic state and the change of impulse due to condensation and heat losses determines the velocity of the gases, see Fig. 9. It decreases downstream, more steeply when the channel gap is thinner.

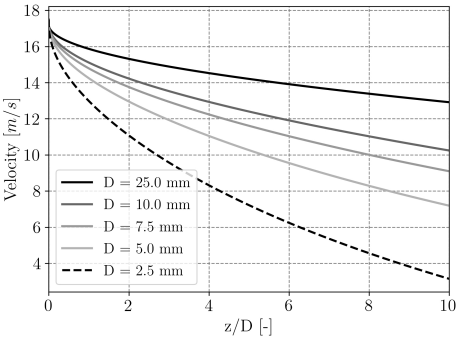

FIG. 9. Velocity of the gaseous products calculated for five gap thicknesses.

In the figures above, we could check the crucial influence of gap thickness in the propagation and condensation of the products. The evolution of pressure, density, temperature and velocity changes correspondingly to the variation of the thickness of the gap.

Further insight of the process can be gained studying the thickness of the liquid layer, Figure 10. This magnitude directly depends on the phase-change function $\dot{m}$. It can be seen that D has a very significant influence in the relative thickness of the liquid layer. In spite of it, the layer remains very thin, of the order of 100 µm, in all conditions.

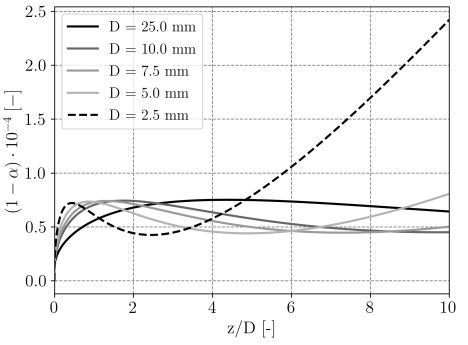

FIG. 10. Dimensionless condensed water film thickness calculated for five gap thicknesses.

Figure 11 contains the percentage of steam that remains in the gaseous phase. This magnitude can be simply estimated as $100\left[(U_G-\dot{z}_f)\rho_G\right] / \left[(U_G|_0-\dot{z}_f)\,\rho_G|_0\right]$. Logically, it follows the opposite trend than $\dot{m}$. Therefore, the initial decrease is very significant as strong condensation exists. This is followed by an ulterior increase, related to the positive values of $\dot{m}$ (*i.e.*, evaporation), that only reaches a local maximum, further decreasing with the distance as condensation takes over and continues downstream.

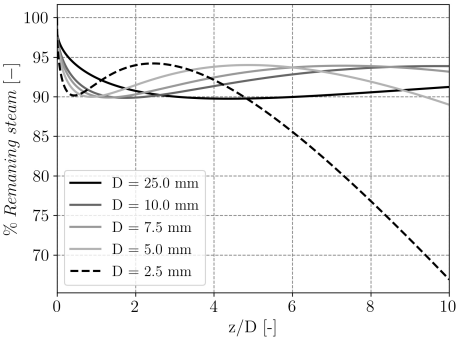

FIG. 11. Percentage of remaining steam in vapour phase.

D. Variable flame propagation velocity $\dot{z}_f$

In the same conditions of the previous parametric study, we consider now a variable $\dot{z}_f$ and a fixed D equal to 10 mm. For the former, we have chosen the values -0.5, -0.75, -1, -1.75, -2.5, -5, -10, $-20\,\mathrm{m\,s^{-1}}$.

We focus on the amount of vapour condensed (Fig. 12). As the flame velocity becomes higher, its value also increases. Even for the larger propagation speed of $\dot{z}_f = -20\,\mathrm{m\,s^{-1}}$ no re-vaporization is seen in the first ten tube diameters. Higher flame velocities result in much higher heat losses through the walls. In the same way, the amount of heat exchanged by the gaseous phase increases, but in a less important manner. Inside of the length of interest, $z/D = 10$, the residence time of the hot gases is reduced when they move faster. Thus, in spite of the stronger heat transfer, the semi-infinite solid constituting the walls only heats up superficially.

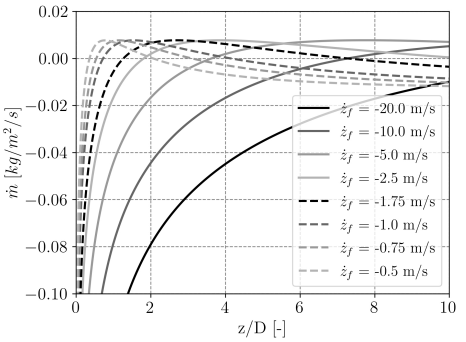

FIG. 12. Amount of vaporized liquid ($\dot{m} > 0$) or condensed vapour ($\dot{m} < 0$) at the chosen domain for five gap thicknesses.

We can observe the effect of the flame velocity on the gas temperature depicted in Fig. 13. The exothermic condensation process heats the gaseous phase, reducing the drop in temperature when faster flames are burned as the change-of-phase rate is higher. In a similar manner, the density increments are much less intense as shown in Fig. 14.

As an additional and general comment on those numerical results we may mention that its accuracy, if needed for practical applications, may be enhanced by adopting a 2D grid for the gas. By this, the transverse heat and mass transfer description in the gas can be significantly improved, while still keeping the interesting simplifications due to the treatment of the condensation.

E. Relation to experimental results

On the right side of Fig. 1, detailed pictures of the flame propagation are shown. The images correspond to the particular motion of near-stoichiometric hydrogen-air premixed

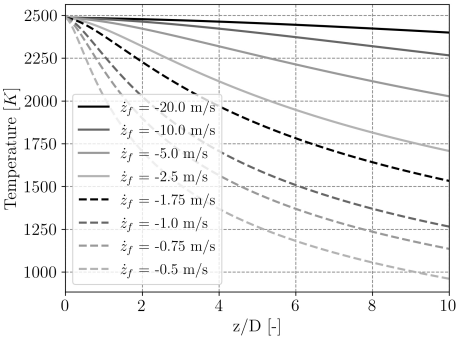

FIG. 13. Temperature of the gaseous products for eight flame propagation velocities.

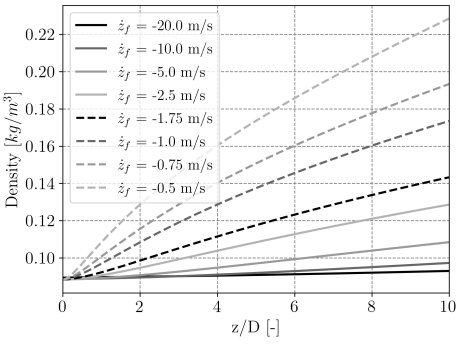

FIG. 14. Density of products for five gap thicknesses.

flames in a 8 mm thick channel. Their dynamics are explained below.

Soon ($z \sim 15$ cm) after ignition, the condensation at the combustion products (dark regions downstream the flame) seems to be strong enough to stop and even change the propagation direction of the front. Likewise, its shape changes when locally moving upwards, showing the characteristic 'V' flame–e.g., the 'double' front obtained from our perspective at $t_0 + 12$ ms–. Later, there appear vaporized areas (lighter regions) around the locations at which this change of direction happens. Finally, once the flame leaves the area of interest, characteristic zebra-like patterns of liquid water remain at the combustion chamber walls.

Therefore, we postulate that condensation-vaporization cycles are the reason of these particular flame dynamics. Note that the *zebra* pattern observed in the experiments is no more that a succession of transparent-opaque areas, and this depending in the existence of condensed water in the walls. It

can be interpreted in terms of the $(1-\alpha)$ variable, as the result of integrating $\dot{m}$, in those situations in which all remaining water, or at least most of it, has been re-vaporized (white areas).

The cyclic behavior appears if an increased flame velocity results in an enhanced condensation of products, and *vice-versa*. This may results in burning velocity oscillations, that happens in a certain period. Under this interpretation, the cyclic dynamics of the process would be: flame acceleration - increase of condensation - deceleration - decrease of condensation - flame acceleration. In terms of the results of section VI D, it could be interpreted as a more pronounced pattern of condensation and re-vaporization as those shown in Figs. 10 or 11. The existence of *loci* at which condensation switches to vaporization see eq. (72) also supports this interpretation. The existence of multiple *loci* of this equation *hints* also such an interpretation with a rich dynamic.

At this stage, we underline that we do not provide or intend to give a comprehensible interpretation of the experiments and merely hint a plausible explanation of them.

VII. CONCLUSIONS

The condensation of combustion products in thin enclosures was formulated using a novel approach, eq. (78). It was derived considering the main characteristics of the condensation problem, namely, the high temperature of the gases and their relatively *fast* motion. Due to this, very thin liquid films appear on the walls of the cavity. Thus allowing us to perform significant simplifications and to carry out an asymptotic expansion.

This results in a compact formulation that, notably, permits to ignore the mere existence of the liquid phase. Consequently, from a physical point of view, the formulation can be understood as an equivalent gaseous tube with permeable walls. Therefore, heat losses to the wall are expressed as a function of the wall characteristics and phase equilibrium temperature only, eq.(54). This can be directly used to calculate the condensation rate $\dot{m}$, eq. (57).

The interpretation of the equation is straightforward. Firstly, the main terms controlling the dynamic are the heat exchange, the mass condensed and its mutual influence. Secondly, friction forces are negligible compared to the condensation rate in most of the domain. Thirdly, the properties of the material of the combustion chamber and the composition of the gaseous mixture–eq. (86)–determine whether condensation appears just behind the flame. Lastly, the characteristic condensation-vaporization-condensation pattern derived theoretically–eq. (72)–is similar to the one found in the experiments.

The model was used to perform parametric studies that show the relative significance of the channel thickness and the flame velocity in the process. Principally, the slenderness of the channel as well as the slowness of the flame exacerbate the condensation significance.

Finally, the construct described by equation (78) has the potential of describing the dynamic of a flame considering the condensation of the products, until now disregarded. This requires the coupling of the model with a 2D-3D flame formulation such as those introduced by[40,43]. Subsequent integration of equation (78), followed by application of the boundary conditions and derivation on time, yields a formulation for $\ddot{z}_f(t)$. That is, the unsteady motion of the reactive front perturbed by the condensation of the combustion products.

DATA AVAILABILITY

The data that support the findings of this study are available from the corresponding author upon reasonable request.

[1]F. Veiga López, *Flame propagation in narrow channels*, Ph.D. thesis, Universidad Carlos III de Madrid (2020).
[2]P. Clavin and G. Searby, *Combustion waves and fronts in flows: flames, shocks, detonations, ablation fronts and explosion of stars* (Cambridge University Press, 2016).
[3]G. I. Sivashinsky, "Instabilities, pattern formation, and turbulence in flames," Annual Review of Fluid Mechanics **15**, 179–199 (1983).
[4]V. Bychkov and M. A. Liberman, "Dynamics and stability of premixed flames," Physics reports **325**, 115–237 (2000).
[5]C. Clanet and G. Searby, "First experimental study of the darrieus-landau instability," Physical review letters **80**, 3867 (1998).
[6]S. Gutman and G. Sivashinsky, "The cellular nature of hydrodynamic flame instability," Physica D: Nonlinear Phenomena **43**, 129–139 (1990).
[7]E. Al Sarraf, C. Almarcha, J. Quinard, B. Radisson, B. Denet, and P. Garcia-Ybarra, "Darrieus–landau instability and markstein numbers of premixed flames in a hele-shaw cell," Proceedings of the Combustion Institute **37**, 1783–1789 (2019).
[8]M. Frankel and G. Sivashinsky, "On the nonlinear thermal diffusive theory of curved flames," Journal de physique **48**, 25–28 (1987).
[9]O. Abidakun, A. Adebiyi, D. Valiev, and V. Akkerman, "Impacts of fuel nonequidiffusivity on premixed flame propagation in channels with open ends," Physics of Fluids **33**, 013604 (2021).
[10]M. Alkhabbaz, O. Abidakun, D. Valiev, and V. Akkerman, "Impact of the lewis number on finger flame acceleration at the early stage of burning in channels and tubes," Physics of Fluids **31**, 083606 (2019).
[11]F. Veiga-López, D. Martínez-Ruiz, E. Fernández-Tarrazo, and M. Sánchez-Sanz, "Experimental analysis of oscillatory premixed flames in a hele-shaw cell propagating towards a closed end," Combustion and Flame **201**, 1–11 (2019).
[12]D. Martínez-Ruiz, F. Veiga-López, and M. Sánchez-Sanz, "Premixed-flame oscillations in narrow channels," Physical Review Fluids **4**, 100503 (2019).
[13]F. Veiga-López, D. Martínez-Ruiz, M. Kuznetsov, and M. Sánchez-Sanz, "Thermoacoustic analysis of lean premixed hydrogen flames in narrow vertical channels," Fuel **278**, 118212 (2020).
[14]R. Sujith and V. R. Unni, "Complex system approach to investigate and mitigate thermoacoustic instability in turbulent combustors," Physics of Fluids **32**, 061401 (2020).
[15]C. Jiménez, D. Fernández-Galisteo, and V. N. Kurdyumov, "Flame-acoustics interaction for symmetric and non-symmetric flames propagating in a narrow duct from an open to a closed end," Combustion and Flame **225**, 499–512 (2021).
[16]H.-J. Kull, "Theory of the rayleigh-taylor instability," Physics reports **206**, 197–325 (1991).
[17]S. M. Ghiaasiaan, *Two-phase flow, boiling, and condensation: in conventional and miniature systems* (Cambridge University Press, 2007).
[18]S. Levy, *Two-phase flow in complex systems* (John Wiley & Sons, 1999).
[19]G. Hetsroni, A. Mosyak, Z. Segal, and E. Pogrebnyak, "Two-phase flow patterns in parallel micro-channels," International Journal of Multiphase Flow **29**, 341–360 (2003).
[20]L. Cheng and D. Mewes, "Review of two-phase flow and flow boiling of mixtures in small and mini channels," International Journal of Multiphase Flow **32**, 183–207 (2006).

[21]J. Xu, P. Cheng, and T. Zhao, "Gas–liquid two-phase flow regimes in rectangular channels with mini/micro gaps," International Journal of Multiphase Flow **25**, 411–432 (1999).
[22]O. C. Jones Jr and J.-M. Delhaye, "Transient and statistical measurement techniques for two-phase flows: a critical review," International Journal of Multiphase Flow **3**, 89–116 (1976).
[23]L. C. Ruspini, C. P. Marcel, and A. Clausse, "Two-phase flow instabilities: A review," International Journal of Heat and Mass Transfer **71**, 521–548 (2014).
[24]J.-M. Delhaye, M. Giot, and M. Riethmuller, *Thermohydraulics of two-phase systems for industrial design and nuclear engineering* (Hemisphere Pub, 1981).
[25]L. Tadrist, "Review on two-phase flow instabilities in narrow spaces," International Journal of Heat and fluid flow **28**, 54–62 (2007).
[26]S. Hayama, "A study on the hydrodynamic instability in boiling channels: 1st report, the instability in a single boiling channel," Bulletin of JSME **6**, 549–556 (1963).
[27]K. Fukuda and T. Kobori, "Classification of two-phase flow instability by density wave oscillation model," Journal of Nuclear science and Technology **16**, 95–108 (1979).
[28]A. Di Benedetto, F. Cammarota, V. Di Sarli, E. Salzano, and G. Russo, "Anomalous behavior during explosions of ch4 in oxygen-enriched air," Combustion and flame **158**, 2214–2219 (2011).
[29]M. Kuznetsov and J. Grune, "Experiments on combustion regimes for hydrogen/air mixtures in a thin layer geometry," International Journal of Hydrogen Energy **44**, 8727–8742 (2019).
[30]I. Martínez, *Termodinamica Basica y aplicada* (DOSAT, 1992).
[31]L. Landau and E. Lifshitz, "Fluid mechanics," Course of theoretical physics **6** (1959).
[32]H. Schlichting, *Boundary layer theory*, Vol. 960 (Springer, 1968).
[33]A. Erdélyi, *Asymptotic expansions* (Courier Corporation, 1956).
[34]T. L. Bergman, F. P. Incropera, D. P. DeWitt, and A. S. Lavine, *Fundamentals of heat and mass transfer* (John Wiley & Sons, 2011).
[35]W. M. Kays, *Convective heat and mass transfer* (Tata McGraw-Hill Education, 2011).
[36]Y. Muzychka and M. Yovanovich, "Laminar forced convection heat transfer in the combined entry region of non-circular ducts," J. Heat Transfer **126**, 54–61 (2004).
[37]A. Bejan and A. D. Kraus, *Heat transfer handbook*, Vol. 1 (John Wiley & Sons, 2003).
[38]A. Bejan, *Convection heat transfer* (John wiley & sons, 2013).
[39]K. Stephan, "Wärmeübergang und druckabfall bei nicht ausgebildeter laminarströmung in rohren und in ebenen spalten," Chemie Ingenieur Technik **31**, 773–778 (1959).
[40]V. N. Kurdyumov and M. Matalon, "Flame acceleration in long narrow open channels," Proceedings of the Combustion Institute **34**, 865–872 (2013).
[41]V. N. Kurdyumov, "Lewis number effect on the propagation of premixed flames in narrow adiabatic channels: Symmetric and non-symmetric flames and their linear stability analysis," Combustion and flame **158**, 1307–1317 (2011).
[42]V. N. Kurdyumov and C. Jiménez, "Propagation of symmetric and non-symmetric premixed flames in narrow channels: Influence of conductive heat-losses," Combustion and flame **161**, 927–936 (2014).
[43]V. N. Kurdyumov and M. Matalon, "Self-accelerating flames in long narrow open channels," Proceedings of the Combustion Institute **35**, 921–928 (2015).
[44]C. Jimenez and V. N. Kurdyumov, "Propagation of symmetric and non-symmetric lean hydrogen–air flames in narrow channels: influence of heat losses," Proceedings of the Combustion Institute **36**, 1559–1567 (2017).
[45]D. Fernández-Galisteo, V. N. Kurdyumov, and P. D. Ronney, "Analysis of premixed flame propagation between two closely-spaced parallel plates," Combustion and Flame **190**, 133–145 (2018).
[46]A. Dejoan, C. Jiménez, and V. N. Kurdyumov, "Critical conditions for non-symmetric flame propagation in narrow channels: Influence of the flow rate, the thermal expansion, the lewis number and heat-losses," Combustion and Flame **209**, 430–440 (2019).
[47]V. Akkerman, C. K. Law, V. Bychkov, and L.-E. Eriksson, "Analysis of flame acceleration induced by wall friction in open tubes," Physics of fluids **22**, 053606 (2010).
[48]D. Valiev, V. Bychkov, V. Akkerman, L.-E. Eriksson, and C. K. Law, "Quasi-steady stages in the process of premixed flame acceleration in narrow channels," Physics of Fluids **25**, 096101 (2013).
[49]V. Bychkov, V. Akkerman, D. Valiev, and C. K. Law, "Influence of gas compression on flame acceleration in channels with obstacles," Combustion and flame **157**, 2008–2011 (2010).
[50]D. Valiev, V. Bychkov, V. Akkerman, C. K. Law, and L.-E. Eriksson, "Flame acceleration in channels with obstacles in the deflagration-to-detonation transition," Combustion and Flame **157**, 1012–1021 (2010).
[51]V. Bychkov, V. Akkerman, G. Fru, A. Petchenko, and L.-E. Eriksson, "Flame acceleration in the early stages of burning in tubes," Combustion and Flame **150**, 263–276 (2007).
[52]D. G. Goodwin, R. L. Speth, H. K. Moffat, and B. W. Weber, "Cantera: An object-oriented software toolkit for chemical kinetics, thermodynamics, and transport processes," `https://www.cantera.org` (2018), version 2.4.0.

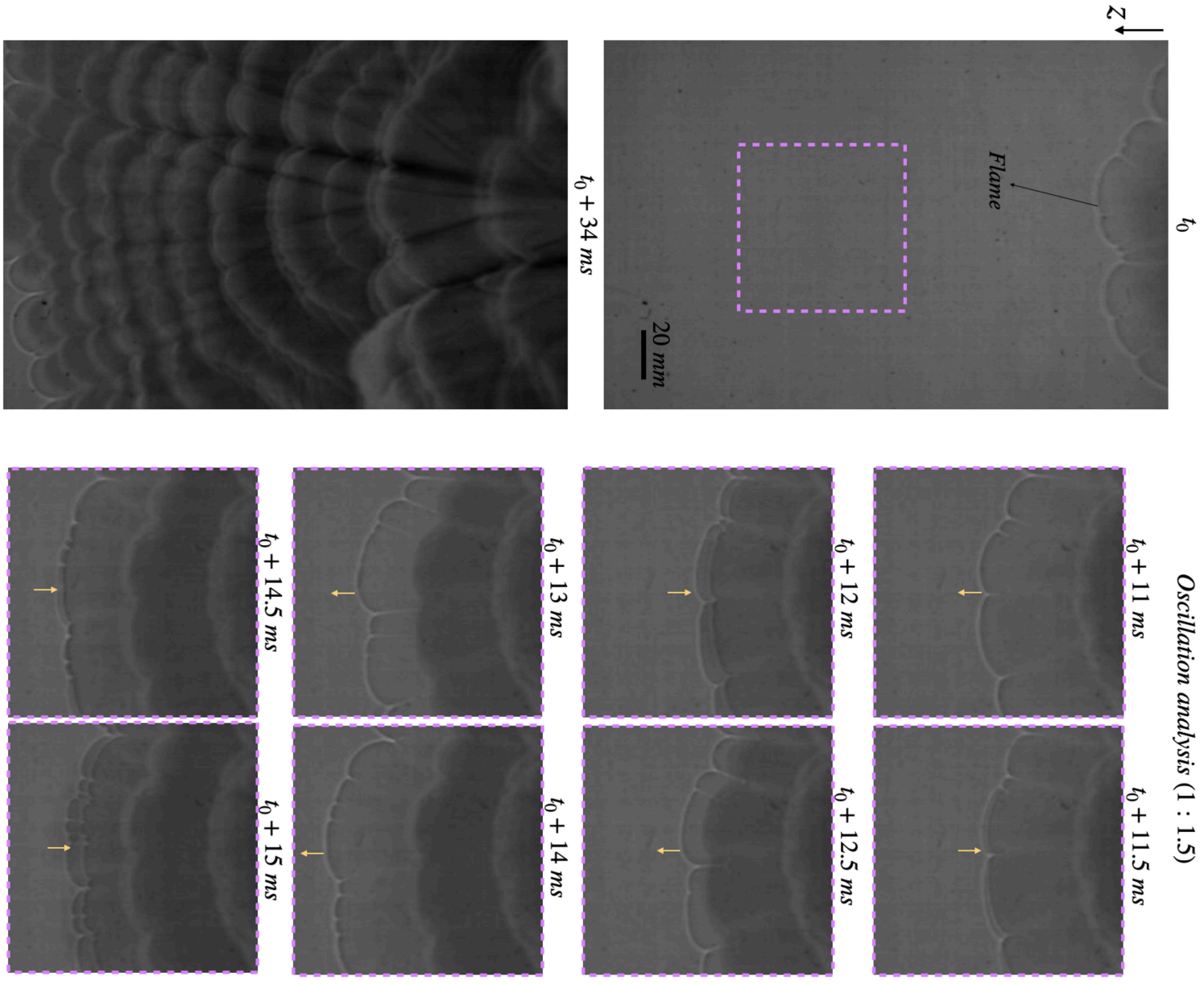

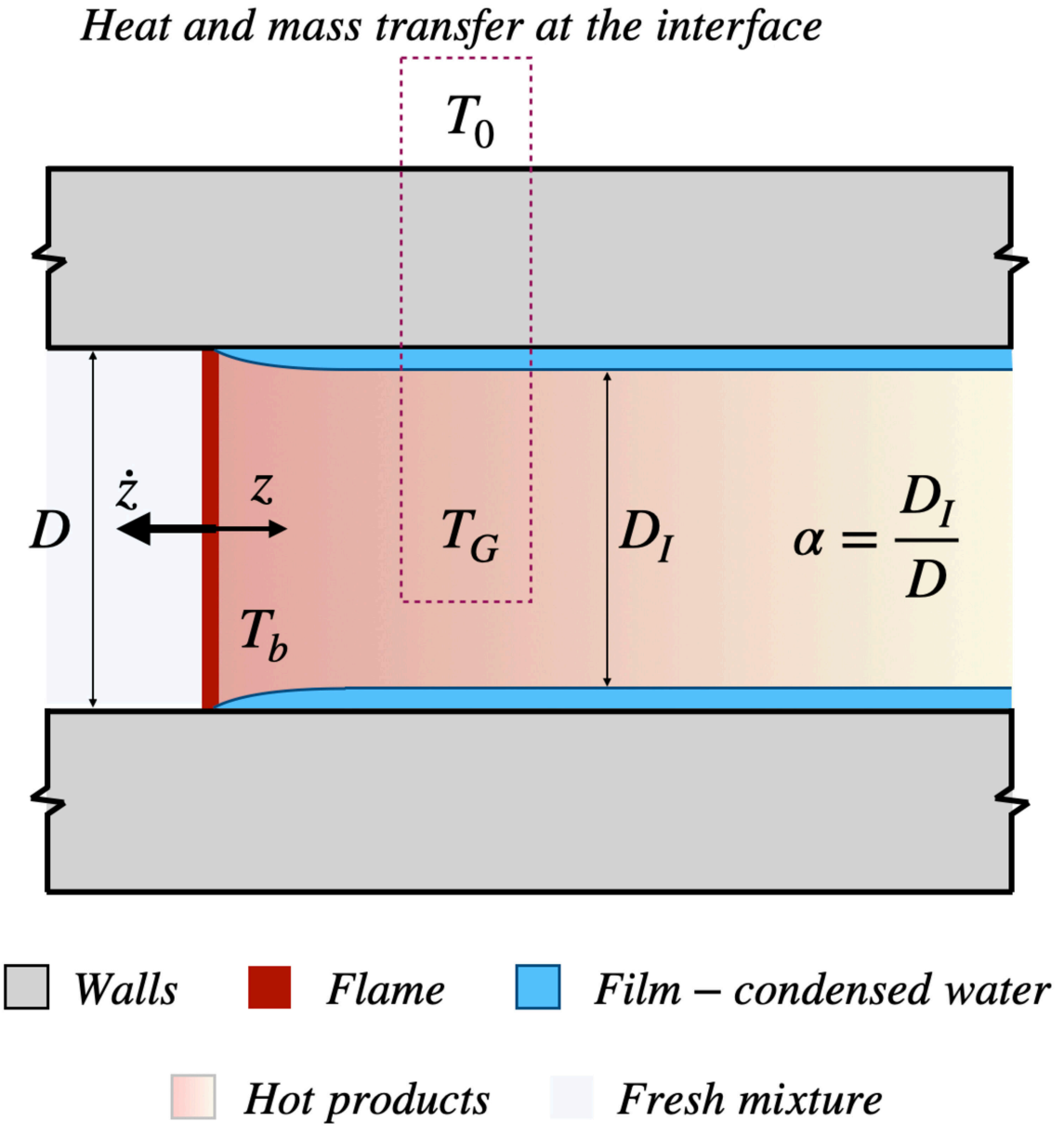

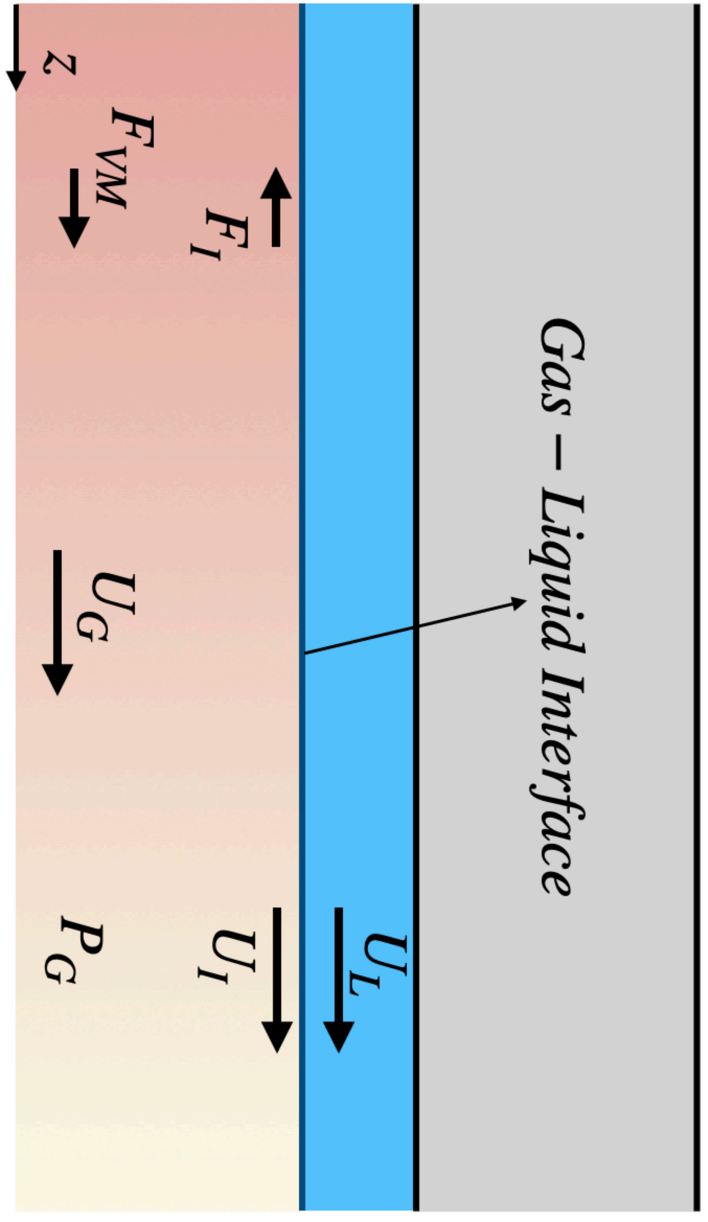

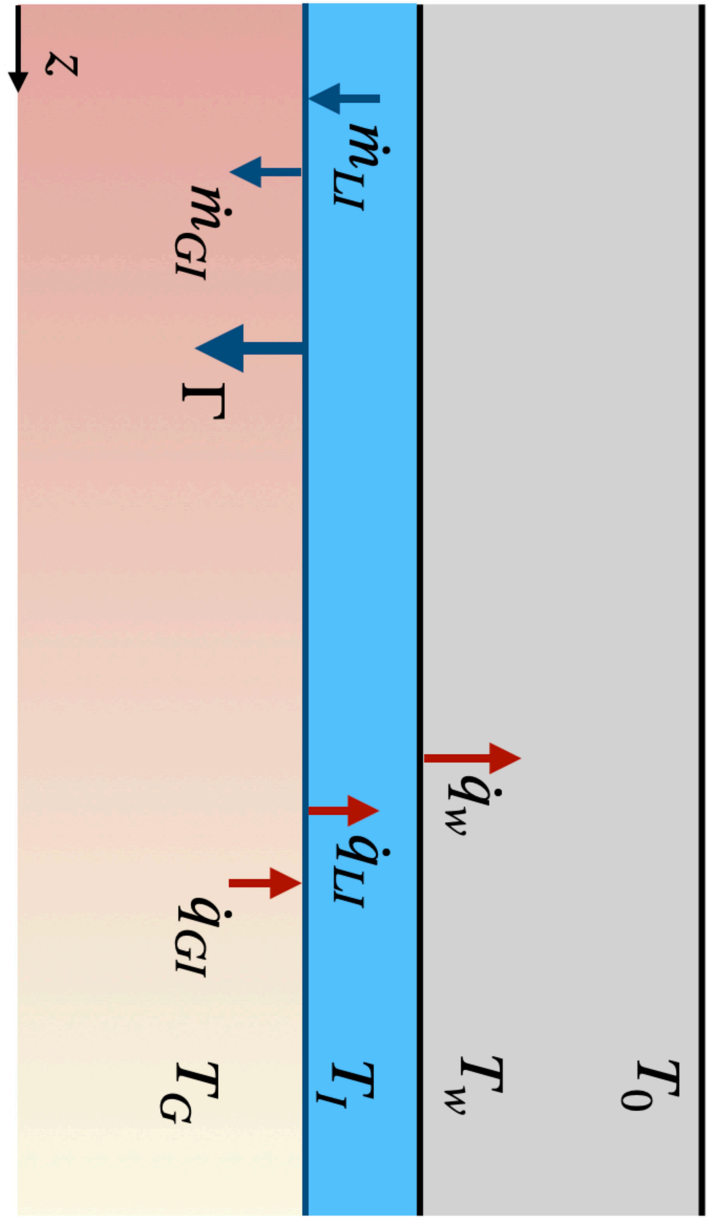

PLEASE CITE THIS ARTICLE AS DOI: 10.1063/5.0056831

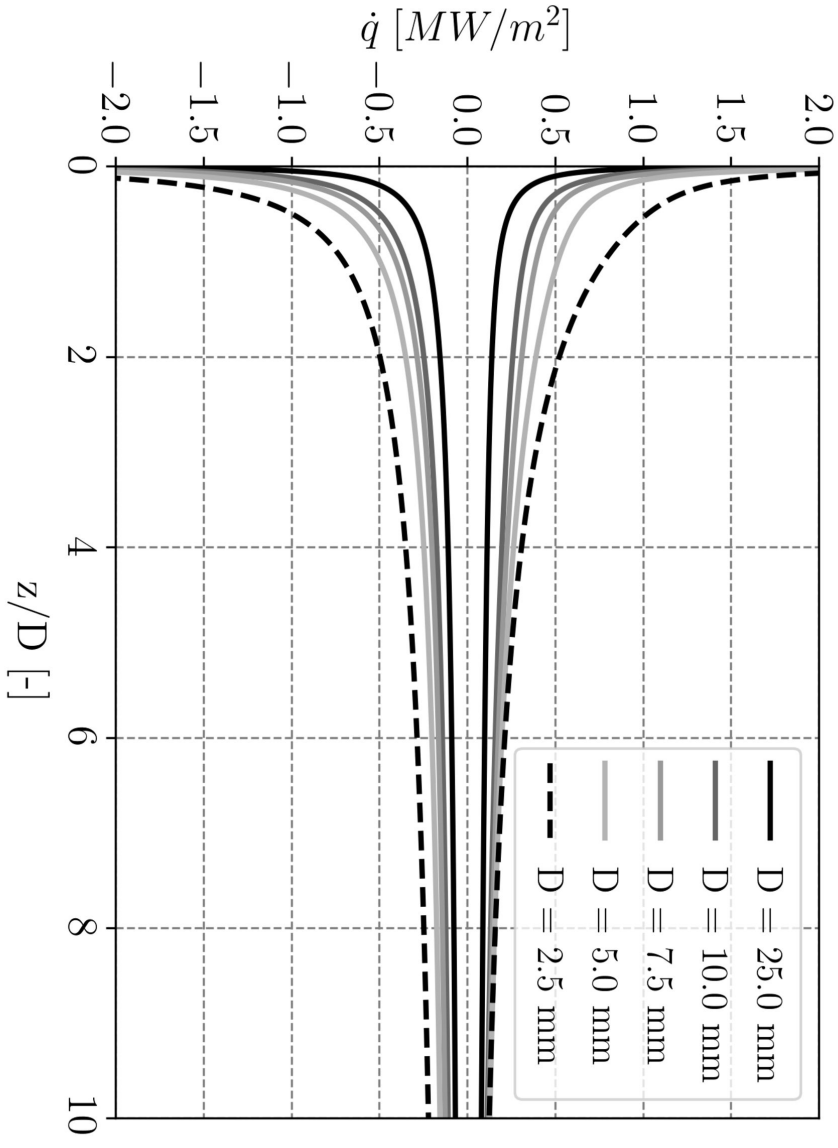

PLEASE CITE THIS ARTICLE AS DOI: 10.1063/5.0056831

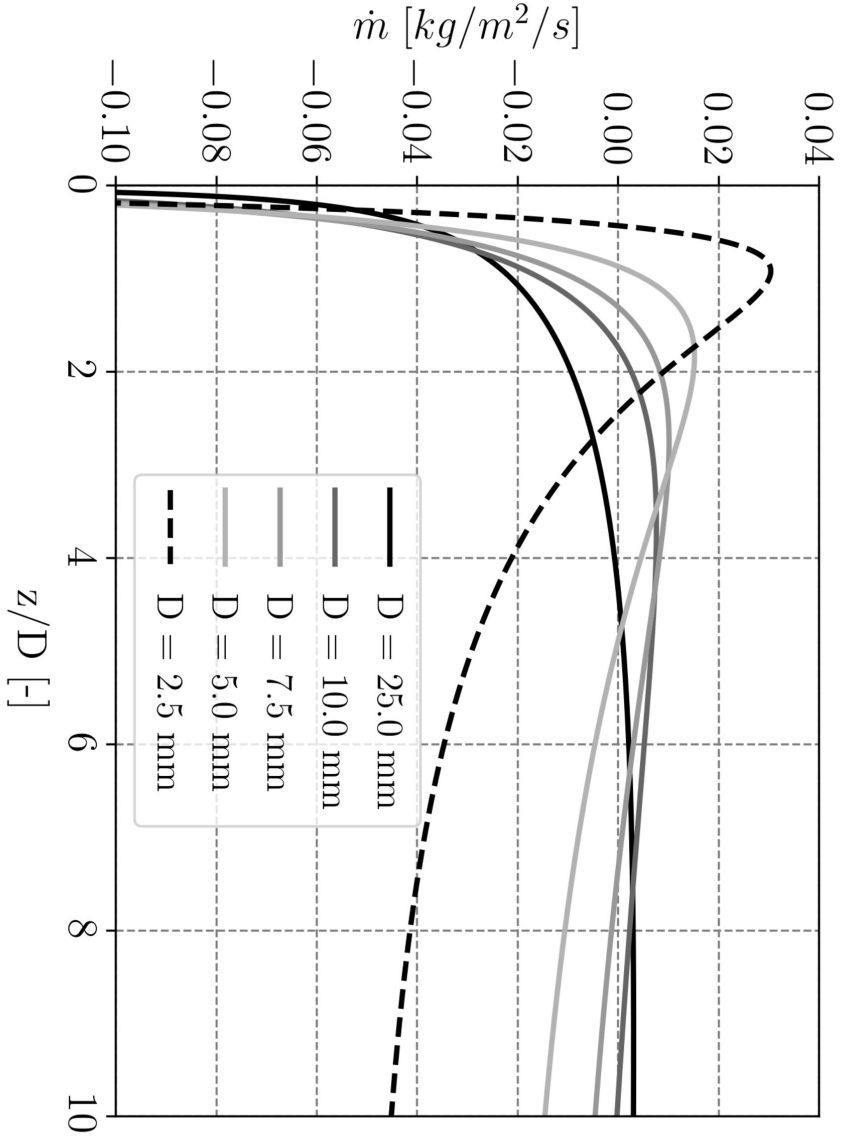

PLEASE CITE THIS ARTICLE AS DOI: 10.1063/5.0056831

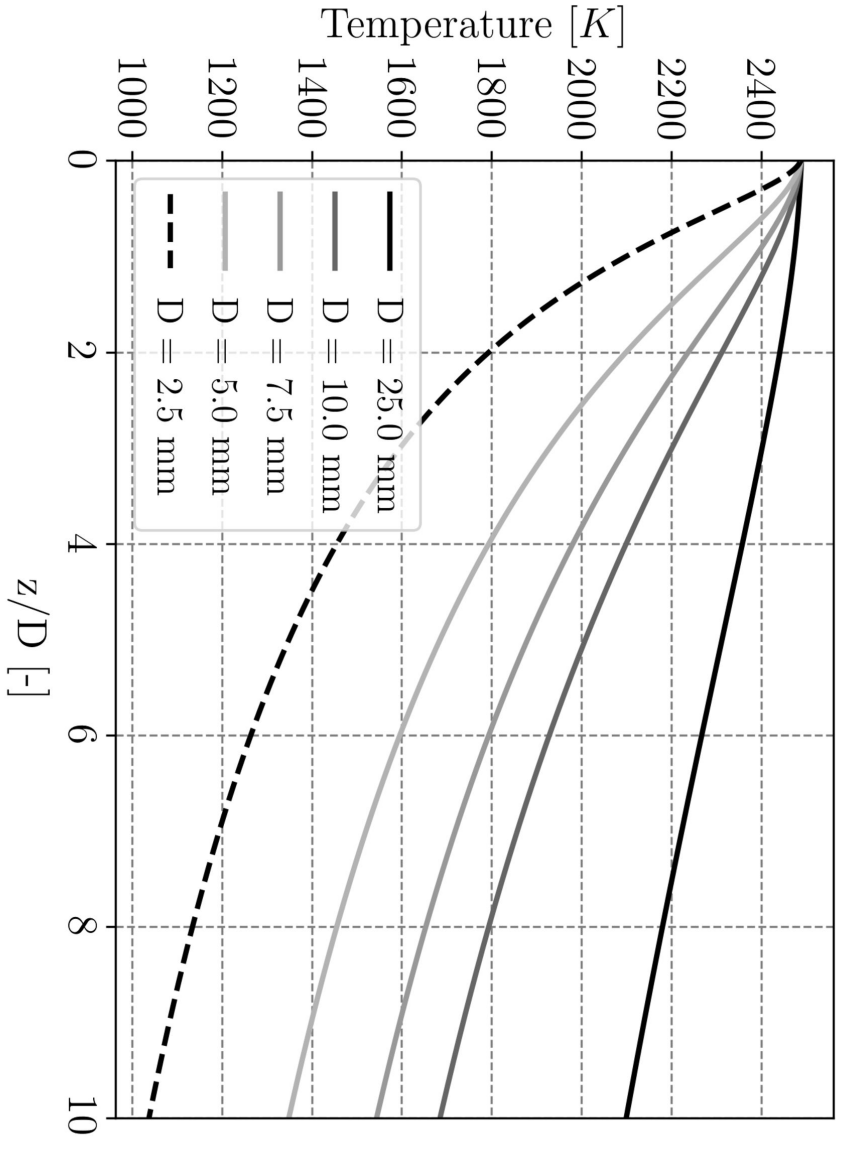

PLEASE CITE THIS ARTICLE AS DOI: 10.1063/5.0056831

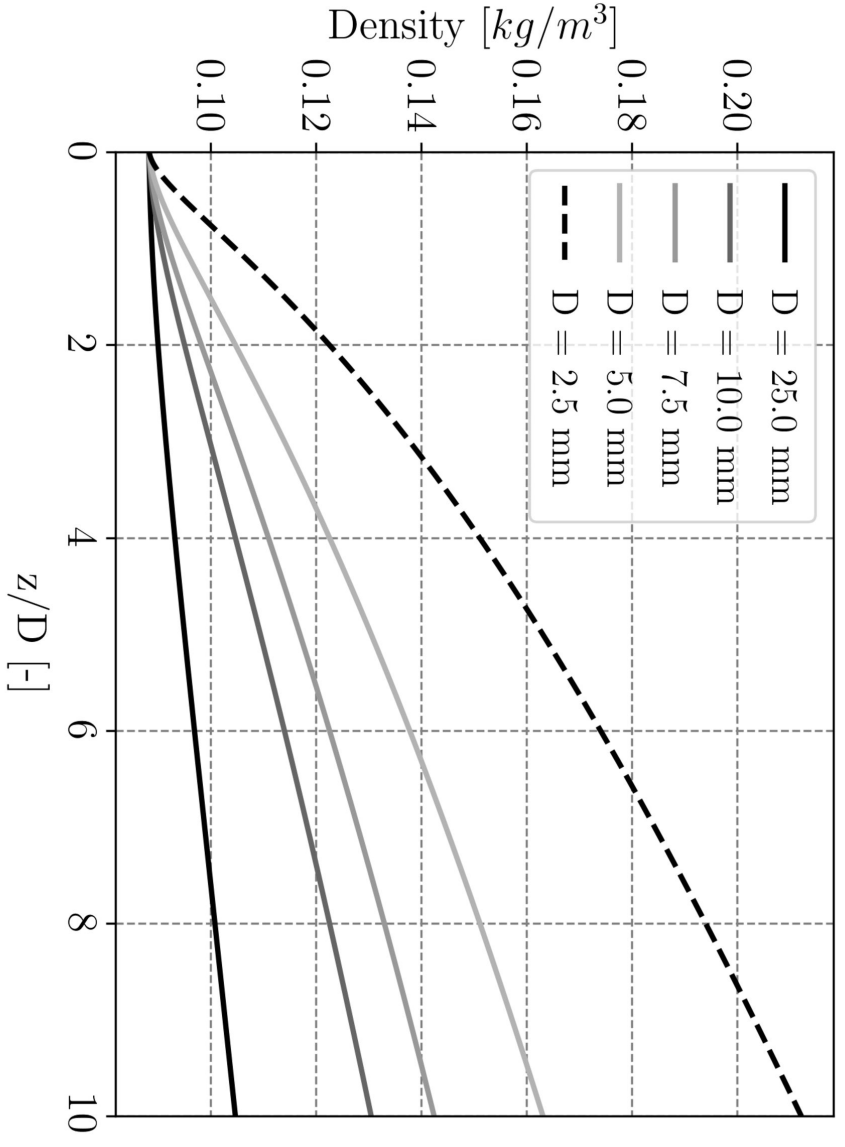

PLEASE CITE THIS ARTICLE AS DOI: 10.1063/5.0056831

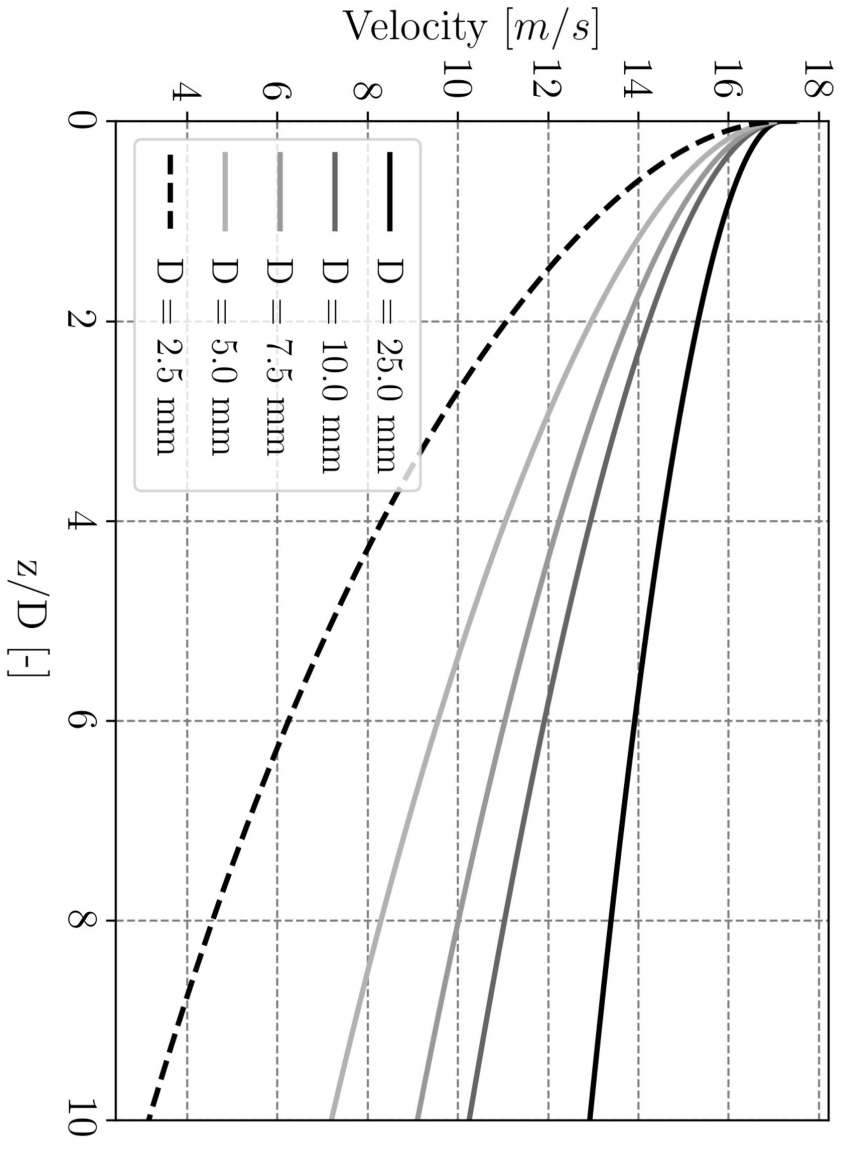

PLEASE CITE THIS ARTICLE AS DOI: 10.1063/5.0056831

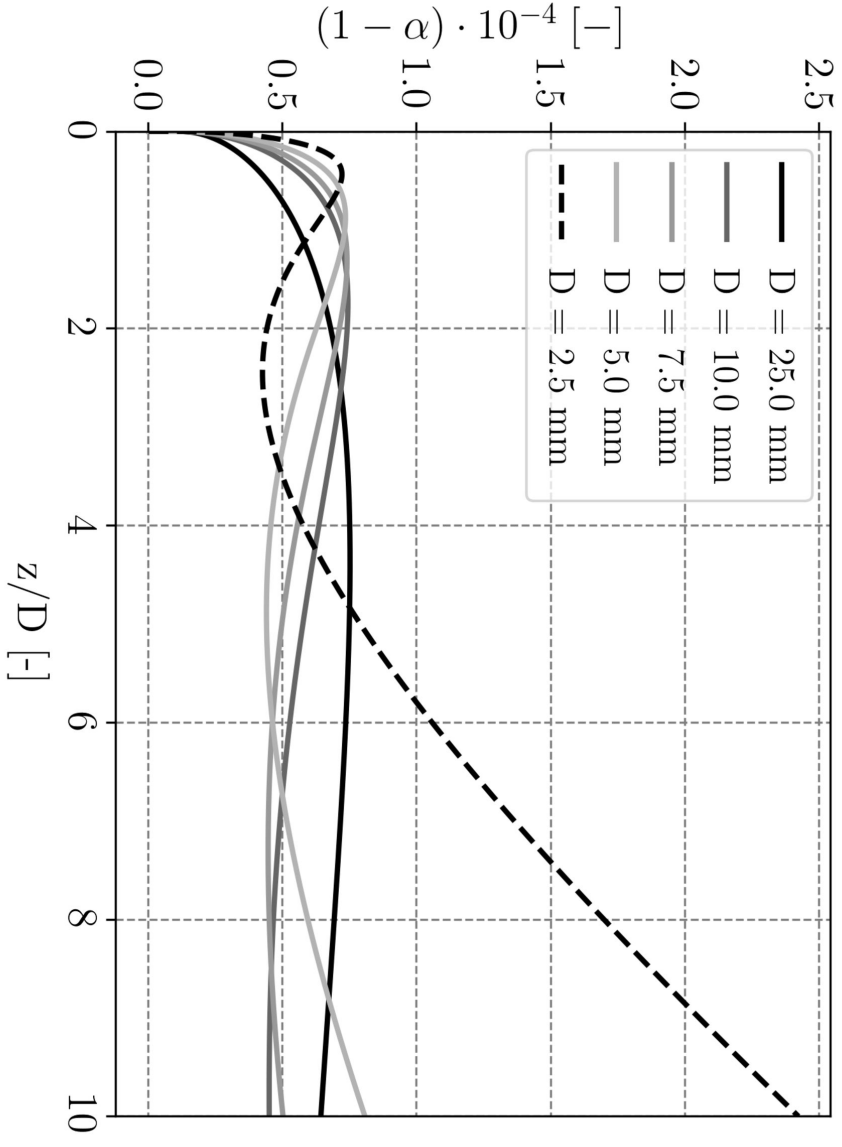

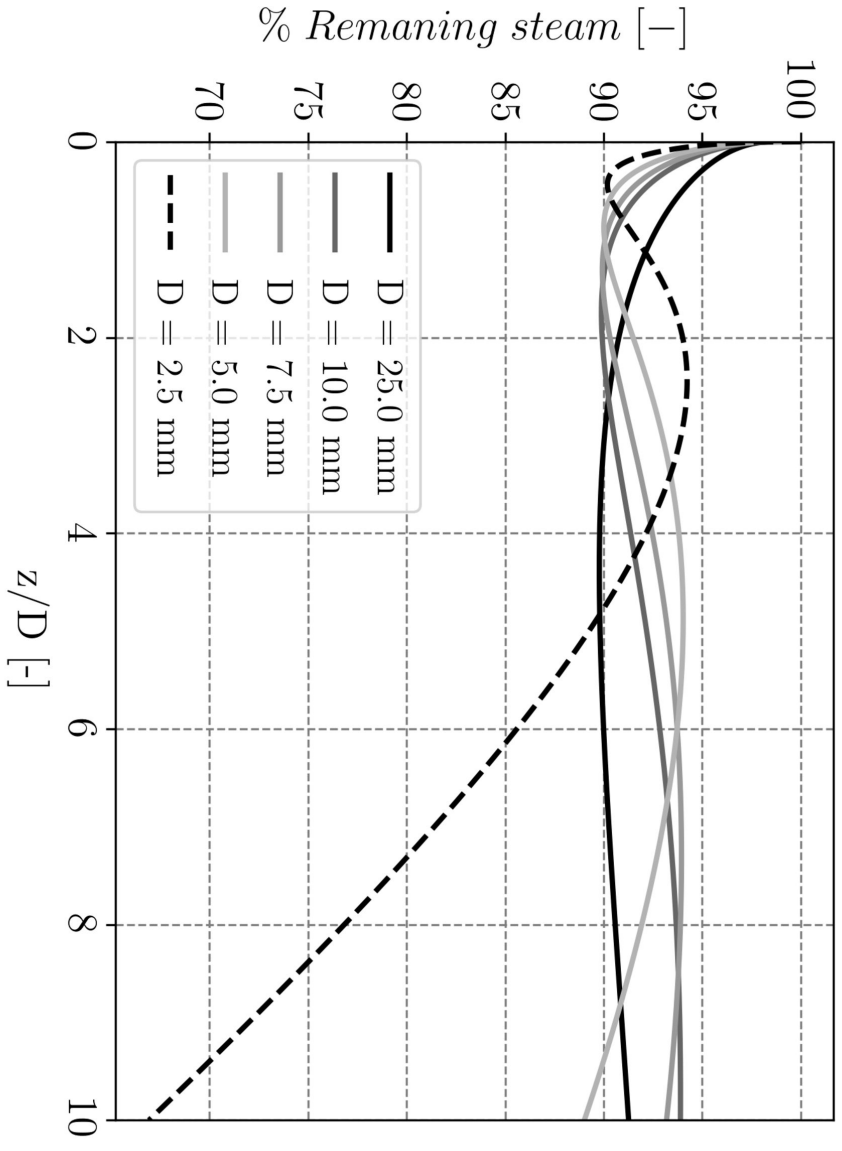

PLEASE CITE THIS ARTICLE AS DOI: 10.1063/5.0056831

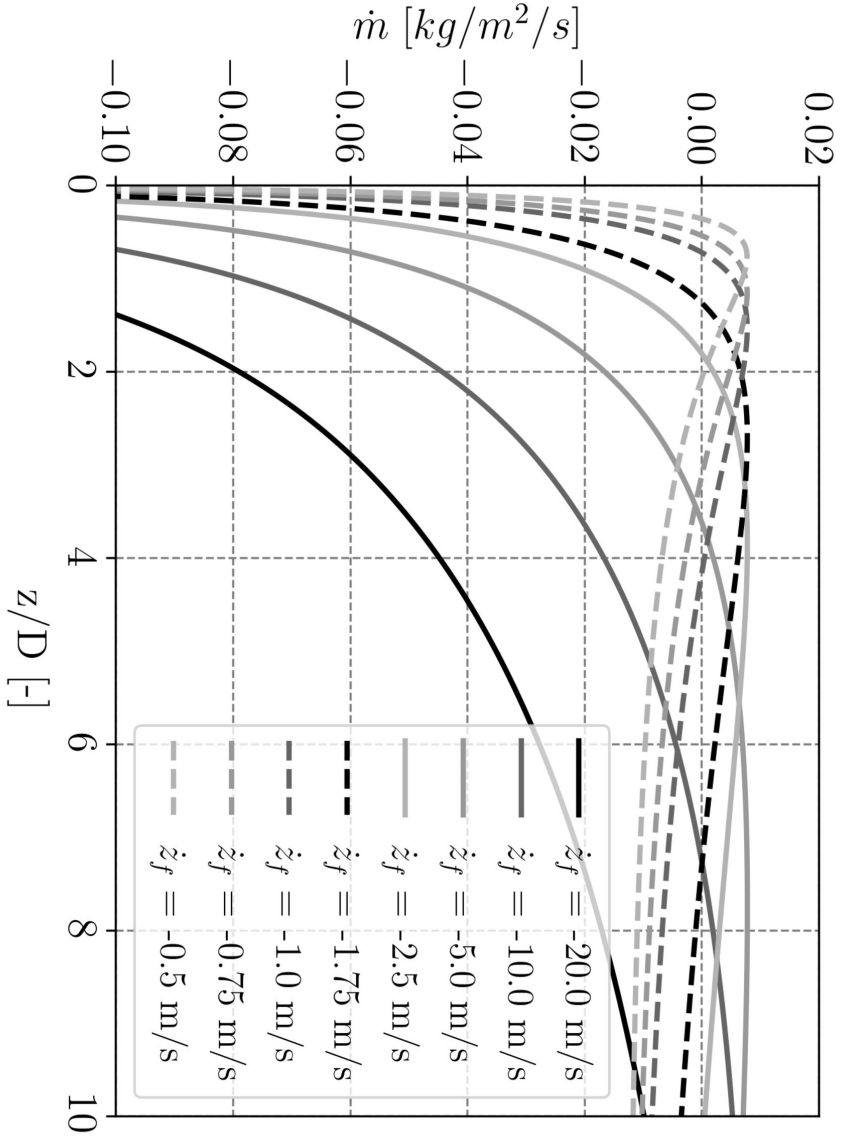

PLEASE CITE THIS ARTICLE AS DOI: 10.1063/5.0056831

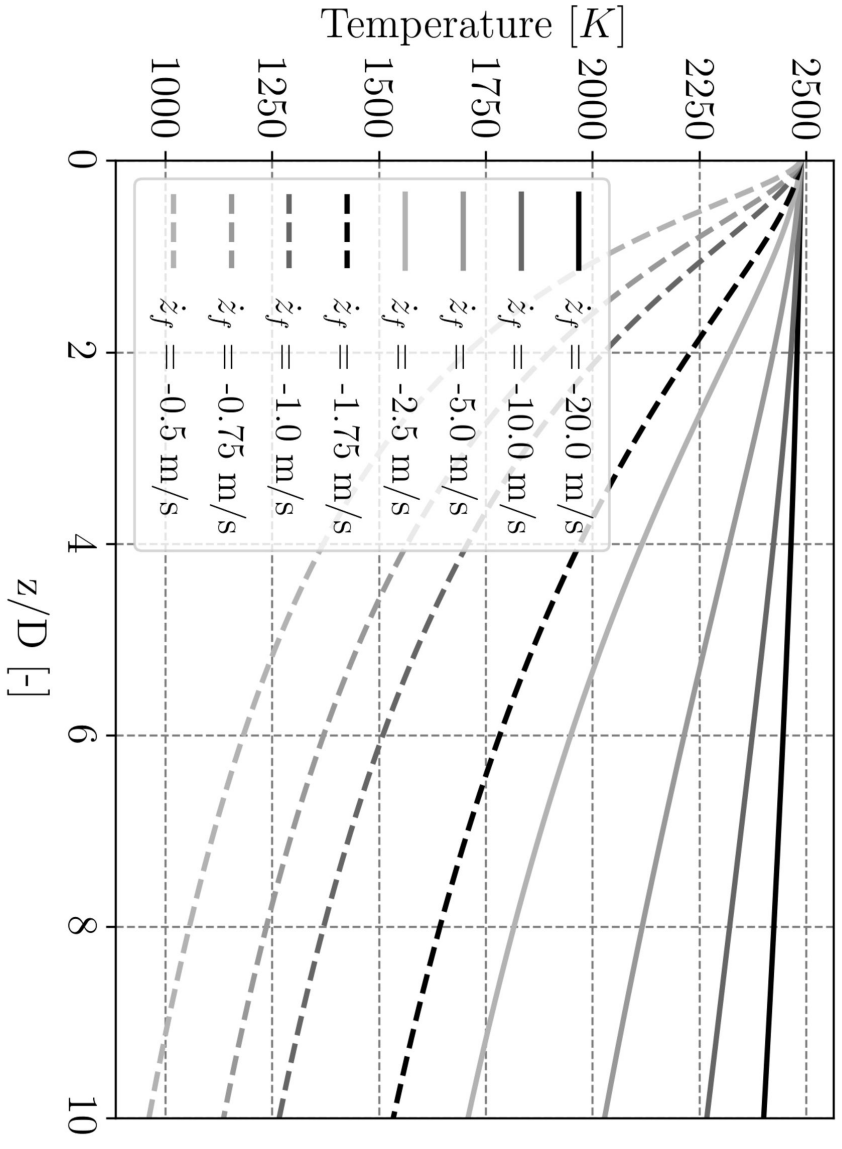

PLEASE CITE THIS ARTICLE AS DOI: 10.1063/5.0056831